

SEGUE 1: AN UNEVOLVED FOSSIL GALAXY FROM THE EARLY UNIVERSE*

ANNA FREBEL¹, JOSHUA D. SIMON², AND EVAN N. KIRBY^{3,4}

ApJ, *accepted*

ABSTRACT

We present Magellan/MIKE and Keck/HIRES high-resolution spectra of six red giant stars in the dwarf galaxy Segue 1. Including one additional Segue 1 star observed by Norris et al., high-resolution spectra have now been obtained for every red giant in Segue 1. Remarkably, three of these seven stars have metallicities below $[\text{Fe}/\text{H}] = -3.5$, suggesting that Segue 1 is the least chemically evolved galaxy known. We confirm previous medium-resolution analyses demonstrating that Segue 1 stars span a metallicity range of more than 2 dex, from $[\text{Fe}/\text{H}] = -1.4$ to $[\text{Fe}/\text{H}] = -3.8$. All of the Segue 1 stars are α -enhanced, with $[\alpha/\text{Fe}] \sim 0.5$. High α -element abundances are typical for metal-poor stars, but in every previously studied galaxy $[\alpha/\text{Fe}]$ declines for more metal-rich stars, which is typically interpreted as iron enrichment from supernova Ia. The absence of this signature in Segue 1 indicates that it was enriched exclusively by massive stars. Other light element abundance ratios in Segue 1, including carbon-enhancement in the three most metal-poor stars, closely resemble those of metal-poor halo stars. Finally, we classify the most metal-rich star as a CH star given its large overabundances of carbon and s-process elements. The other six stars show remarkably low neutron-capture element abundances of $[\text{Sr}/\text{H}] < -4.9$ and $[\text{Ba}/\text{H}] < -4.2$, which are comparable to the lowest levels ever detected in halo stars. This suggests minimal neutron-capture enrichment, perhaps limited to a single r-process or weak s-process synthesizing event. Altogether, the chemical abundances of Segue 1 indicate no substantial chemical evolution, supporting the idea that it may be a surviving first galaxy that experienced only one burst of star formation.

Subject headings: early universe — galaxies: dwarf — Galaxy: halo — Local Group — stars: abundances — stars: Population II

1. INTRODUCTION

The early phases of the chemical evolution of the Universe can be reconstructed through the study of metal-poor stars. Given their low metallicity, these stars are assumed to have formed in the early Universe. Since then, these long-lived stars have locked up information on the properties of their birth gas clouds and the local chemical and physical conditions in their atmospheres that can be extracted through spectroscopic analysis.

Metal-poor stars in the halo of the Milky Way have thus been used for decades to unravel the chemical enrichment history of the Galaxy (e.g., McWilliam et al. 1995; Beers & Christlieb 2005; Frebel & Norris 2013). In this way the Galaxy has been found to be chemically diverse, with multiple populations and components, and to contain a variety of substructure. These signatures clearly show how closely the chemical evolution of a galaxy is connected to its assembly history. But it is difficult to cleanly uncover the various astrophysical pro-

cesses that have been involved in element nucleosynthesis and star formation in the Milky Way over billions of years. Dwarf galaxies, however, being smaller systems with presumably simpler formation histories, provide the means to study chemical enrichment in a more straightforward way. At the same time, comparison of their population of metal-poor stars with those in the Milky Way provides insight into the assembly of the Galactic halo.

In the last decade, the Sloan Digital Sky Survey (SDSS) transformed our picture of the Milky Way's satellite galaxy population. The wide sky coverage and sufficiently deep photometry revealed dwarf galaxies with total luminosities ranging from 300 to $10^5 L_{\odot}$ (e.g., Willman et al. 2005; Zucker et al. 2006; Belokurov et al. 2007; Martin et al. 2008). These new galaxies were found not only to be unprecedentedly faint but also unprecedentedly dominated by dark matter (Simon & Geha 2007). Nonetheless, they form a continuous sequence of stellar mass with the classical dwarf spheroidal galaxies in terms of star formation history (Brown et al. 2012), structural properties (Okamoto et al. 2012), and metal content (Kirby et al. 2008, 2011a).

A significant challenge to study individual stars in these dwarf galaxies in great detail is the difficulty in achieving the spectral data quality required for chemical abundance analyses (e.g., Koch et al. 2008; Frebel et al. 2010b; Simon et al. 2010). Most dwarf galaxies orbit dozens of kpc away in the outer halo and their brightest stars therefore have typical apparent magnitudes of $V = 17$ to 18. However, high-resolution spectroscopy is required to investigate the detailed stellar abundance patterns that reflect various enrichment events, and such

* This paper includes data gathered with the 6.5 meter Magellan Telescopes located at Las Campanas Observatory, Chile. Data herein were also obtained at the W. M. Keck Observatory, which is operated as a scientific partnership among the California Institute of Technology, the University of California, and NASA. The Observatory was made possible by the generous financial support of the W. M. Keck Foundation.

¹ Kavli Institute for Astrophysics and Space Research and Department of Physics, Massachusetts Institute of Technology, Cambridge, MA 02139, USA

² Observatories of the Carnegie Institution of Washington, Pasadena, CA 91101, USA

³ Center for Galaxy Evolution, Department of Physics and Astronomy, University of California, Irvine, CA 92697, USA

⁴ Center for Galaxy Evolution Fellow

spectra can only be obtained for faint stars with long integrations on the largest telescopes available. Accordingly, relatively small numbers of stars in most of the classical dwarf spheroidal (dSph) galaxies with $10^5 L_\odot \lesssim L \lesssim 10^7 L_\odot$ and the ultra-faint dwarfs ($L \lesssim 10^5 L_\odot$) have been observed at high spectral resolution.

1.1. *The chemical evolution of dwarf galaxies and the Milky Way*

In the Milky Way it is well known that low-metallicity halo stars ($[\text{Fe}/\text{H}] < -1.0$) have enhanced abundances of the α -elements (e.g., Edvardsson et al. 1993), while at higher metallicities the $[\alpha/\text{Fe}]$ ratios smoothly approach the solar ratio (e.g., Tinsley 1979; McWilliam 1997; Venn et al. 2004). The canonical interpretation of this behavior is that it reflects the timescales of nucleosynthesis from different kinds of supernovae. Massive stars produce large amounts of the α -elements both during their stellar evolution and in their explosions as core collapse supernovae. These elements are quickly returned to the interstellar medium because the lifetimes of such stars are short, less than 10 Myr. Type Ia supernovae, which primarily produce iron, do not begin exploding until a poorly known delay time (typically assumed to be of order 10^8 yr; Maoz & Mannucci 2012) has elapsed since an episode of star formation. The $[\alpha/\text{Fe}]$ plateau at $[\text{Fe}/\text{H}] < -1.0$ then corresponds to the epoch when only core-collapse supernovae contributed significantly to the overall nucleosynthesis, and the decline to $[\alpha/\text{Fe}] = 0$ occurs when Type Ia supernovae begin occurring in significant numbers as well.

The turnover from the high $[\alpha/\text{Fe}]$ plateau in the classical dSph galaxies occurs at lower metallicity than in the Milky Way, $[\text{Fe}/\text{H}] \sim -2.5$ (e.g., Tolstoy et al. 2003; Venn et al. 2004), revealing that they have been enriched on slower timescales than what is observed in the halo of the Galaxy (see e.g., Tolstoy et al. 2009 for a review). Note that, at least in the case of Sagittarius, McWilliam et al. (2013) have questioned whether this explanation for the decline in $[\alpha/\text{Fe}]$ at high metallicity is correct, and they suggest a top-light initial mass function (IMF) as an alternative.

More recently, Kirby et al. (2008, 2011b) measured metallicities for dozens of individual stars in ultra-faint dwarfs using the medium-resolution spectroscopy from Simon & Geha (2007). Stars with metallicities of $[\text{Fe}/\text{H}] < -3.0$ were uncovered in surprisingly large relative numbers, whereas essentially no stars with $[\text{Fe}/\text{H}] > -1.0$ were found. This general characteristic of overall metal-deficiency correlates with the low luminosities of these galaxies. They extend the metallicity-luminosity relationship for dSph galaxies by several orders of magnitude in luminosity (Kirby et al. 2008, 2011c, 2013). Vargas et al. (2013) then used the same spectra to measure $[\alpha/\text{Fe}]$ abundance ratios. They found that among their sample of eight ultra-faint dwarfs, only Segue 1 does not show declining $[\alpha/\text{Fe}]$ ratios with increasing metallicity⁶. Thus, this galaxy is the only dwarf galaxy known

to have minimal chemical enrichment from Type Ia supernovae.

However, medium-resolution spectroscopy is limited in its ability to detect and measure the abundances of some elements, such as the neutron-capture elements. High-resolution spectroscopy can provide highly detailed abundance information for stars that are bright enough. High-resolution spectra with large wavelength coverage of stars down to magnitude of $V \sim 19.2$ have been obtained for about a dozen stars in ultra-faint dwarfs by now. Three stars each in Ursa Major II and Coma Berenices were observed by Frebel et al. (2010b), Koch et al. (2008) observed two stars in Hercules, and other studies reported on one star each in Leo IV (Simon et al. 2010), Boötes I (Norris et al. 2010c), Segue 1 (Norris et al. 2010a), and the stream passing just in front of Segue 1 that may have originated in an ultra-faint dwarf (Frebel et al. 2013b).

Detailed studies of these stars, nearly all of which are at $[\text{Fe}/\text{H}] \lesssim -2.0$, revealed close-to-identical chemical abundance patterns compared with halo stars, both in terms of the abundance ratios as well as more global population signatures such as a significant fraction of metal-poor stars being strongly enhanced in carbon relative to iron, and showing low neutron-capture element abundances. It has thus been suggested that the chemical similarity of halo and the ultra-faint dwarf galaxy stars could be due to the stars having formed from early gas that was enriched in the same fashion, i.e., exclusively by massive stars (Frebel et al. 2010b; Simon et al. 2010; Norris et al. 2010c,a). Moreover, if the surviving ultra-faint dwarf galaxies had earlier analogs that were accreted by the Milky Way in its early assembly phases, the chemical similarity of halo and dwarf galaxy stars could also be interpreted as indicating that the early enrichment history of the destroyed dwarfs closely resembled that of the surviving dwarfs observed today, despite the different environments they formed in. In this picture, very low luminosity primordial dwarfs may have provided the now-observed metal-poor “halo” stars to the halo.

In this context, it is interesting to note that the analysis of deep *HST* color-magnitude diagrams of three ultra-faint dwarf galaxies, Hercules, Leo IV, and Ursa Major I, by Brown et al. (2012) shows that they are at least as old as the oldest globular clusters and likely nearly as old as the Universe itself (their age is consistent with that of the globular cluster M92, which on the same scale is measured at 13.7 Gyr). Preliminary results for three additional ultra-faint dwarfs suggest that the stellar populations of all six galaxies are indistinguishable (Brown et al. 2013). This demonstrates that the metal-poor stars in these galaxies are as old as their chemical composition (galaxy average metallicities range from $[\text{Fe}/\text{H}] \sim -2.0$ to -2.6 ; Kirby et al. 2008) suggests. Because of the apparently small age spreads in these systems, their more metal-rich stars also have to be similarly old, suggesting rapid enrichment. This could be due to the low-mass nature of these systems which would lead to a fast, significant build up of metals after only a few supernova explosions. Considering a plausible chemical composition of a first galaxy that may have survived to the present day, Frebel & Bromm (2012) thus

UMa II.

⁶ Figure 4 in Vargas et al. (2013) indicates that UMa II contains a single metal-rich ($[\text{Fe}/\text{H}] \sim -1.0$) and α -enhanced ($[\alpha/\text{H}] \sim 0.4$) star that might place it in this category as well. However, high-resolution spectroscopy of this star by Frebel et al. (2010b) showed that it is actually a foreground star rather than a member of

argued that Segue 1 (together with Ursa Major II, Coma Berenices, Boötes I, and Leo IV) are candidate systems for such surviving first galaxies. Bovill & Ricotti (2011) agree that most of the ultra-faint dwarfs are consistent with expectations for reionization fossils, although they do not place Segue 1 in this category as a result of earlier estimates of its metallicity lying above the luminosity-metallicity relation established by brighter dwarfs. The metallicities derived in this paper and improved measurements of the L–Z relation by Kirby et al. (2013) demonstrate that Segue 1 is in fact consistent with the extrapolated metallicity–luminosity relationship of more luminous systems. Only additional chemical abundance data for more stars in as many of the ultra-faint dwarfs as possible will allow detailed tests of the hypothesis that these objects are fossils of the first galaxies by establishing a detailed account of the chemical composition of each galaxy.

Thus, in this study we present chemical abundance measurements for six stars in Segue 1 that are just bright enough to be observable with high-resolution spectroscopy. Segue 1 is the faintest galaxy yet detected, and it has an average metallicity of $[\text{Fe}/\text{H}] \sim -2.5$ to -2.7 (Norris et al. 2010b; Simon et al. 2011). It was one of five new ultra-faint galaxies discovered by Belokurov et al. (2007) using a matched filter search of SDSS DR5 and SEGUE photometry. Although Segue 1 contains very few stars, its position 50° out of the Galactic plane and away from the Galactic center aids in separating member stars from the foreground Milky Way population. It is also close enough (23 kpc) to permit spectroscopy of stars down to ~ 1 mag below the main sequence turnoff (e.g., Geha et al. 2009; Simon et al. 2011). Segue 1 was initially presumed to be a globular cluster because of its small half-light radius (30 pc), but Geha et al. (2009) presented a strong case based on internal stellar kinematics that Segue 1 is highly dark matter-dominated and therefore a galaxy. Geha et al. (2009) also demonstrated that Segue 1 lies on or near standard dwarf galaxy scaling relations. Niederste-Ostholt et al. (2009) found photometric evidence for tidal debris near Segue 1 and proposed that the velocity dispersion of Segue 1 was inflated by contamination from these disrupted structures, but Simon et al. (2011) showed that contamination is unlikely and that the measured velocity dispersion is robust. The extensive spectroscopy by both Simon et al. (2011) and Norris et al. (2010b) also established that Segue 1 has metallicity spreads of 0.7 to 0.8 dex in $[\text{Fe}/\text{H}]$ and 1.2 dex in $[\text{C}/\text{H}]$. Along with being extremely underluminous and the most dark matter-dominated and lowest-metallicity object currently known, Segue 1 is not only a galaxy, but perhaps the most extreme galaxy known.

With our new observations, our aim is to quantify the chemical evolution of this galaxy by constraining its enrichment processes. This way, we can learn about the limited star formation that occurred in this early system. In § 2 we describe the observations and in § 3 our analysis techniques. We interpret our chemical abundance results (§ 4) within the context of early galaxy formation and chemical evolution in § 5. We conclude in § 6.

2. OBSERVATIONS

2.1. Target selection

The first spectroscopy of Segue 1 was obtained by Geha et al. (2009), who used medium resolution Keck/DEIMOS spectra to identify 24 member stars of the galaxy, including a single red giant for which they estimated $[\text{Fe}/\text{H}] = -3.3$. Simon et al. (2011) followed up this study by observing an essentially complete spectroscopic sample (again with Keck/DEIMOS) out to 2.3 half-light radii around Segue 1 and down to a magnitude limit of $r = 21.7$ (~ 1 mag below the main sequence turnoff). The Simon et al. (2011) survey identified five additional members on the Segue 1 red giant branch (RGB), and a total of 71 member stars. Independently, Norris et al. (2010b) used medium resolution blue spectra from AAOmega on the Australian Astronomical Telescope (AAT) over a much wider field to search for bright Segue 1 members. They found four of the same RGB stars as Simon et al. (2011), as well as another extremely metal-poor (EMP) giant, Segue 1-7, nearly four half-light radii from the center of the galaxy. One other candidate RGB member from the Norris et al. (2010b) sample, Segue 1-42, was found by Simon et al. (2011) to have a radial velocity inconsistent with membership in Segue 1, while the last (and faintest) RGB candidate identified by Norris et al., Segue 1-270, is unlikely to be a genuine member given its location ~ 10 half-light radii from Segue 1 and its velocity offset of $\sim 20 \text{ km s}^{-1}$ from the systemic velocity.

As a result of these extensive observations and the remarkably puny stellar population of the galaxy, the seven known RGB stars are likely to represent a complete inventory of all stars in Segue 1 currently in the red giant phase of evolution (it also has two horizontal branch stars; Simon et al. 2011). For a Plummer radial profile, 10% of member stars should be located at projected radii beyond three half-light radii, within which the Simon et al. (2011) sample is more than 90% complete. In fact, two of the seven giants (29%) are beyond this distance, suggesting that the present sample includes most (if not all) of the RGB stars in Segue 1. Norris et al. (2010a) obtained a high-resolution VLT spectrum of the brightest giant star, Segue 1-7, and analyzed its unusual chemical inventory, confirming its extremely low metallicity and carbon enhancement. As described below, we have now obtained high resolution spectra of the remaining six Segue 1 giants, including two stars with $[\text{Fe}/\text{H}] < -3.5$ and two others at $[\text{Fe}/\text{H}] > -1.8$ that are the most metal-rich stars in an ultra-faint dwarf galaxy to be studied in detail.

2.2. High-resolution spectroscopy

We observed five of our six target stars with the MIKE spectrograph (Bernstein et al. 2003) on the Magellan-Clay telescope in March and May 2010, and March 2011. Observing conditions during these runs were mostly clear, with an average seeing of $0.8''$ to $1.0''$. Additional details of the MIKE observations are given in Table 1. MIKE spectra have nearly full optical wavelength coverage from ~ 3500 – 9000 \AA . A $1.0'' \times 5''$ slit yields a spectral resolution of $\sim 22,000$ in the red and $\sim 28,000$ in the blue wavelength regime. We used 2×2 on-chip binning and the $1.0''$ slit for all stars except SDSS J100639+160008. The seeing conditions were bet-

ter when we began observing this star, so we opted to employ a $0.7'' \times 5''$ slit. It yields a resolution of $\sim 28,000$ and $\sim 35,000$, respectively.

Integration times ranged from ~ 6 to 15 h. The observations were typically broken up in 55 min exposures to avoid significant degradation of the spectra by cosmic rays. These individual spectra generally had low counts given the faintness of the objects, with little or no flux detected below 4000 Å.

We observed the final star in the sample, SDSS J100742+160106, with the HIRES spectrograph (Vogt et al. 1994) on the KeckI telescope on 2010 April 1. The observations were obtained with a $1.15'' \times 7''$ slit (providing a spectral resolution of 37,500), the kv389 blocking filter, and a total integration time of 3.6 h. The autoguider had difficulty guiding accurately during much of this time, initially because of unusually good seeing conditions and later as the star transited within a few degrees of the zenith, so many of the exposures were either unguided or employed manual guiding by the telescope operator. These guiding issues decreased the S/N of some exposures, but should not have any effect on the measurement of equivalent widths we are interested in for the purposes of this paper. We reduced the HIRES spectra using the IDL pipeline developed by J. X. Prochaska and collaborators⁷.

Reductions of the individual MIKE spectra were carried out using the MIKE Carnegie Python pipeline initially described by Kelson (2003)⁸. The orders of the combined spectrum were normalized and merged to produce final one-dimensional blue and red spectra for further analysis. The S/N of the spectra is modest and ranges from 20 to 40 at ~ 5300 Å and 30 to 50 at ~ 6000 Å. Radial velocity measurements yield values between 200 and 208 km s⁻¹, which are consistent with previous measurements (Simon et al. 2011).

In Figure 1 we show representative portions of the spectra of the program stars around the Ba line at 4554 Å and the Mg b lines at 5170 Å. The large range of metallicities found in Segue 1 is easily visible. For comparison we also add CD -38 245 with $[\text{Fe}/\text{H}] \sim -4.2$ as well as Arcturus ($[\text{Fe}/\text{H}] = -0.5$), which bracket the metallicities of our Segue 1 stars.

3. CHEMICAL ABUNDANCE ANALYSIS

3.1. Line measurements

We measured the equivalent widths of metal absorption lines throughout the spectra by fitting Gaussian profiles to them. Continuum placement was challenging at times given the modest S/N of the data. Generally, lines between 4000 Å and 7000 Å were measured, based on a linelist described in Roederer et al. (2008). In Table 2, we list the lines used and their measured equivalent widths for all elements, and 3σ upper limits for selected elements. For blended lines, lines with hyperfine-structure (HFS), and molecular features such as CH, we used the spectral synthesis approach in which the abundance of a given species is obtained by matching the observed spectrum to a synthetic spectrum of known abundance.

In many instances the element abundances were so low that no absorption lines could be detected. The modest S/N of the data also made detections of weak lines difficult. This was the case for all neutron-capture elements in all our stars except the most metal-rich object and the Ba measurements in SDSS J100742+160106 (see Section 4.4). We determined upper limits through spectrum synthesis by matching synthetic spectra to the noise level in the region of the non-detected absorption line. These generally agree well with calculations for 3σ upper limits.

3.2. Stellar parameters

We use 1D plane-parallel model atmospheres with α -enhancement from Castelli & Kurucz (2004) and the latest version of the MOOG analysis code (Snedden 1973; Sobeck et al. 2011). The abundances are computed under the assumption of local thermodynamic equilibrium (LTE). We calculated final abundance ratios $[\text{X}/\text{Fe}]$ using the solar abundances of Asplund et al. (2009). The elemental abundances for our sample are given in Table 6.

To derive stellar parameters spectroscopically we follow the procedure described in Frebel et al. (2013a). For completeness we repeat essential details below. We derive spectroscopic effective temperatures by demanding that there be no trend of Fe I line abundances with excitation potential. We use initial temperature guesses based on the shape of the Balmer lines. Using the ionization balance, i.e., demanding that Fe I lines yield the same abundance as Fe II lines, we derive the surface gravity, $\log g$, for all sample stars. The microturbulence, v_{micr} , is obtained iteratively in this process by demanding no trend of abundances with reduced equivalent widths.

However, this spectroscopic technique is known to deliver cooler temperatures (and lower surface gravities) than those derived from photometry, especially for cool giants (see e.g., Hollek et al. 2011 for a discussion). To alleviate this effect, we thus applied temperature adjustments of $T_{\text{eff,corrected}} = T_{\text{eff,initial}} - 0.1 \times T_{\text{eff,initial}} + 670$ as presented in Frebel et al. (2013a) after obtaining the spectroscopic parameters. This relation was derived from the analysis of seven well-studied stars in the literature for which photometric temperatures were available. We then repeated determining the stellar parameters spectroscopically but with the adjusted temperature fixed while finding the new, corresponding $\log g$ and v_{micr} . We estimate our temperature uncertainties to be $\sim 100 - 150$ K (see also Frebel et al. 2010b as well as Section 4.5 for more details on uncertainties). Uncertainties in $\log g$ and v_{micr} are estimated to be 0.3 dex and 0.3 km s⁻¹. Finally, we visually inspect the shape of the Balmer lines to confirm the temperatures. Compared to other stars with known temperatures, our derived values are in qualitative agreement with the shapes of the Balmer lines for those temperatures. Having available stellar temperatures that are not as discrepant from photometric temperatures makes subsequent abundance comparisons with other stars more straightforward. Another advantage of the spectroscopic approach over photometric temperatures is that it is reddening-independent (although Segue 1 has only moderate reddening of $E(B - V) \sim 0.03$ mag).

Figure 2 shows our final stellar parameters in comparison with α -enhanced ($[\alpha/\text{Fe}] = 0.3$) 12 Gyr isochrones (Green et al. 1984; Kim et al. 2002) covering a range of

⁷ <http://www.ucolick.org/~xavier/HIReflux/index.html>

⁸ Available at <http://obs.carnegiescience.edu/Code/python>

TABLE 1
OBSERVING DETAILS

Star	α (J2000)	δ (J2000)	UT dates	slit	t_{exp} hr	g mag	$E(B - V)$ mag	S/N 5300 Å	S/N 6000 Å
SDSS J100714+160154	10 07 14.6	+16 01 54.5	2011-03-10	1.0''	5.5	18.86	0.027	35	45
SDSS J100710+160623	10 07 10.1	+16 06 23.9	2011-03-13/22	1.0''	7.3	19.20	0.026	28	45
SDSS J100702+155055	10 07 02.5	+15 50 55.3	2011-03-11/12	1.0''	9.2	18.50	0.033	35	46
SDSS J100742+160106	10 07 42.7	+16 01 06.9	2010-04-01	1.15''	3.6	18.60	0.027	20	30
SDSS J100652+160235	10 06 52.3	+16 02 35.8	2010-03-07/08/18/19/23/24	1.0''	15	18.89	0.029	42	50
SDSS J100639+160008	10 06 39.3	+16 00 08.9	2010-03-18/19/22, 2010-05-08/09	0.7''	8	19.48	0.031	26	33

NOTE. — The S/N is measured per ~ 33 mÅ pixel (MIKE spectra) and ~ 20 mÅ pixel (HIRES spectrum).

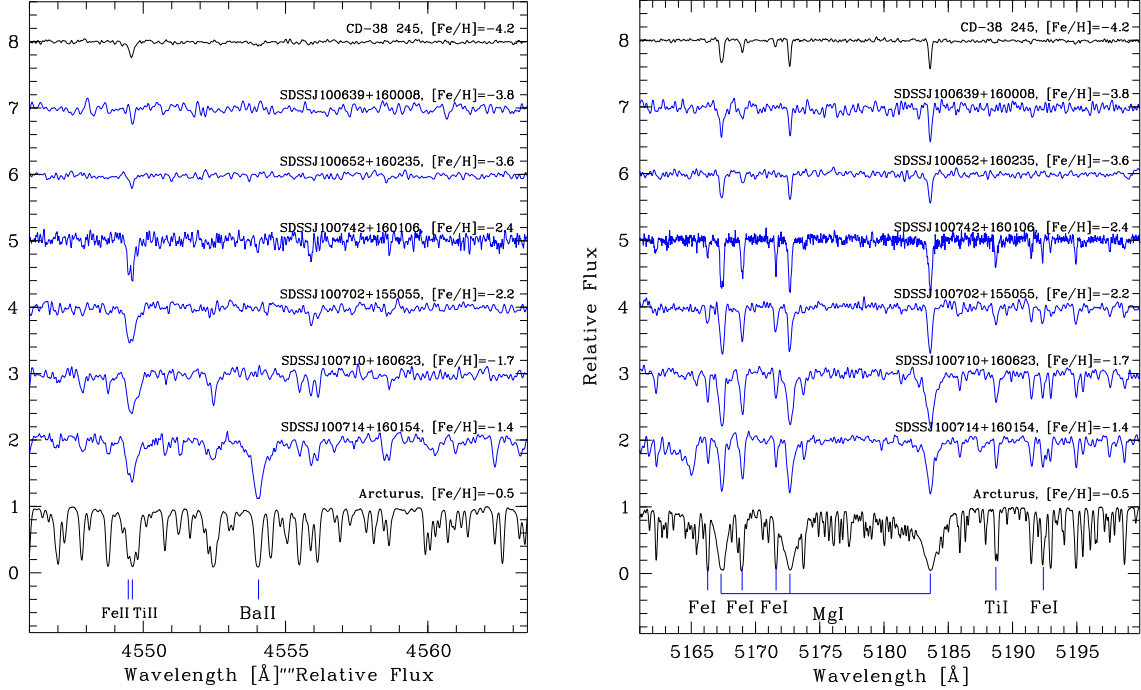


FIG. 1.— Magellan/MIKE and Keck/HIRES spectra of our Segue 1 sample stars, shown near the Ba II line at 4554 Å (left panel) and near the Mg b lines around 5180 Å (right panel). Some absorption lines are indicated. The stars are bracketed in terms of their metallicity by the Arcturus (bottom) and CD -38 245 (top) spectra, to illustrate the large metallicity spread in Segue 1. The Ba II line is only detected in two stars, indicating that Segue 1 is deficient in neutron-capture elements.

metallicities. Our values agree very well with those of the isochrone. Table 3 lists the individual stellar parameters of all stars. For completeness we added Segue 1-7, the other star in Segue 1 that was observed at high spectral resolution by Norris et al. (2010a).

Given the modest S/N of the spectra, we note that relatively few iron lines are measured, especially for Fe II. In the case of the two most metal-poor stars, no Fe II lines for the gravity determination were confidently detected. We thus chose gravity values from the isochrone appropriate for their effective temperatures. We note, however, that upper limits on the Fe II lines (taken at face value) would yield gravities within 0.5 dex of the adopted values. This suggests that our final surface gravities, which place them on the red giant branch rather than the horizontal branch, are reasonable choices (see also below).

We also used published equivalent width measurements from Norris et al. (2010a) to obtain stellar parameters and abundances for Segue 1-7 in the same way as for our other Segue 1 stars. The agreement with the values they

determined is very good. We find $T_{\text{eff}} = 4990$ K, $\log g = 2.05$, $v_{\text{micr}} = 1.35$ km s $^{-1}$ and $[\text{Fe}/\text{H}] = -3.55$, compared to 4960 K, 1.9, 1.3 km s $^{-1}$ and -3.57 (Norris et al. 2010a).

We show the available SDSS photometry in Figure 3 in the form of a color-magnitude diagram overlaid with an M92 fiducial sequence and a HB track from M13. g magnitudes and reddening are also listed in Table 1. Overall, the location of the stars on the giant branch in the photometry is confirmed with the stellar spectroscopic parameters. We note that the $g - i$ color of SDSS J100639+160008 from the Sloan Digital Sky Survey is slightly offset from the best-fitting Segue 1 isochrone by ~ 0.1 mag to the blue; since this offset disappears in other colors (e.g., $g - r$ and $r - z$), it could indicate an error in the SDSS i magnitude. Since this star has the lowest metallicity in the sample we were not able to determine its surface gravity spectroscopically because no Fe II lines were detected. However, we explicitly checked whether we could have obtained a slightly

TABLE 2
EQUIVALENT WIDTH MEASUREMENTS OF THE SEGUE 1 STARS (TABLE WILL BE AVAILABLE ELECTRONICALLY)

El.	λ [Å]	χ [eV]	$\log gf$ [dex]	EW [mÅ] SDSS J100714+160154	$\lg \epsilon$ [dex]	EW [mÅ] SDSS J100710+160623	$\lg \epsilon$ [dex]	EW [mÅ] SDSS J100702+155055	$\lg \epsilon$ [dex]	EW [mÅ] SDSS J100742+160106	$\lg \epsilon$ [dex]	EW [mÅ] SDSS J100652+160106	$\lg \epsilon$ [dex]
CH	4313	syn	...	syn	6.86	syn	6.19	syn	5.83	syn	...
CH	4325	syn	8.45	syn	6.96	syn	6.19	syn	6.03	syn	...
Na I	5889.950	0.00	0.108	240.13	4.67	190.82	4.26	148.77	3.86	118.78	3.59	59.86	...
Na I	5895.924	0.00	-0.194	228.99	4.90	171.68	4.36	146.43	4.13	104.38	3.63	49.00	...
Mg I	3829.355	2.71	-0.208	105.97	...
Mg I	3832.304	2.71	0.270	149.84	...
Mg I	3986.753	4.35	-1.030	136.44	6.79	41.40	5.57	45.98	5.71
Mg I	4057.505	4.35	-0.890	115.68	6.52	102.39	6.39	52.37	5.61	58.80	5.79
Mg I	4167.271	4.35	-0.710	147.70	6.72	113.51	6.41	66.83	5.66
Mg I	4351.906	4.34	-0.525	16.32	...
Mg I	4571.096	0.00	-5.688	97.38	6.76	107.88	6.50	73.71	5.97	60.04	5.91
Mg I	4702.990	4.33	-0.380	164.91	6.33	138.89	6.22	101.58	5.76	90.03	5.70	19.85	...
Mg I	5172.684	2.71	-0.450	232.36	5.62	234.66	5.74	107.33	...
Mg I	5183.604	2.72	-0.239	278.54	5.64	265.44	5.68	129.87	...
Mg I	5528.405	4.34	-0.498	134.62	6.37	136.80	6.44	98.01	5.91	75.26	5.66
Mg I	5711.090	4.34	-1.724	43.80	6.42
Al I	3944.006	0.00	-0.620	syn	4.32	syn	...	syn	3.23	syn	3.25	syn	...
Al I	3961.520	0.01	-0.340	247.13	4.40	174.31	3.88	125.58	3.35	127.09	3.50
Si I	3905.523	1.91	-1.092	syn	syn	5.50	syn	...
Si I	4102.936	1.91	-3.140	105.50	6.48	113.95	6.37	77.71	5.70	74.36	5.74
Ca I	4226.730	0.00	0.244	265.88	4.37	107.11	...
Ca I	4283.010	1.89	-0.224	111.60	5.25	72.35	4.42	60.08	4.31
Ca I	4318.650	1.89	-0.210	107.79	5.26	114.04	5.28	77.30	4.51	68.49	4.48
Ca I	4425.440	1.88	-0.358	119.08	5.42	93.72	4.93	63.37	4.35	66.32	4.54
Ca I	4434.960	1.89	-0.010	151.22	5.42	128.04	5.17	87.98	4.48	80.80	4.50	21.10	...
Ca I	4435.690	1.89	-0.519	114.08	5.53	119.19	5.56	56.50	4.40	49.81	4.39
Ca I	4454.780	1.90	0.260	122.48	4.83	95.19	4.35	84.41	4.32	30.80	...
Ca I	4455.890	1.90	-0.530	107.68	5.46	85.79	4.96	56.50	4.42	48.44	4.38
Ca I	5262.244	2.52	-0.471	69.05	5.44	82.30	5.53	37.75	4.69	30.01	4.60
Ca I	5265.556	2.52	-0.260	87.74	5.58	92.17	5.53	51.83	4.74	34.25	4.48
Ca I	5349.465	2.71	-0.310	66.48	5.40	54.69	5.01
Ca I	5581.971	2.52	-0.555	57.28	5.30	56.77	5.09
Ca I	5588.760	2.52	0.210	90.42	5.15	113.00	5.45	76.34	4.72	55.30	4.44
Ca I	5590.120	2.52	-0.571	61.09	5.18
Ca I	5594.468	2.52	0.097	101.48	5.46	103.69	5.38	61.23	4.55	55.69	4.56
Ca I	5598.487	2.52	-0.087	98.27	5.60	44.09	4.51
Ca I	5601.285	2.53	-0.523	70.54	5.52	83.71	5.61	23.51	4.50
Ca I	5857.450	2.93	0.230	74.60	5.22	104.57	5.66	46.62	4.59	37.19	4.49
Ca I	6102.720	1.88	-0.790	89.77	5.33	97.94	5.32	61.91	4.71	43.81	4.49
Ca I	6122.220	1.89	-0.315	122.40	5.30	128.35	5.32	75.06	4.48	62.66	4.39
Ca I	6162.170	1.90	-0.089	127.87	5.14	137.20	5.21	97.77	4.65	87.03	4.63
Ca I	6169.055	2.52	-0.797	50.03	5.35	58.09	5.32
Ca I	6169.559	2.53	-0.478	68.77	5.36	71.70	5.27	32.35	4.58	21.25	4.39
Ca I	6439.070	2.52	0.470	106.71	5.14	106.07	5.01	77.16	4.46	62.95	4.32
Ca I	6449.810	2.52	-0.502	59.62	5.26	46.06	4.81	21.45	4.34	29.90	4.61
Ca I	6499.649	2.52	-0.818	49.14	5.39	55.81	5.31
Ca I	6717.685	2.71	-0.524	53.55	5.32	61.51	5.31	28.48	4.73
Sc II	4246.820	0.32	0.240	syn	1.53	syn	1.48	syn	0.86	syn	1.11	syn	...
Sc II	4314.083	0.62	-0.100	syn	1.88	syn	0.80	syn	1.05	syn	...
Sc II	4324.998	0.59	-0.440	syn	1.68	syn	1.00	syn	1.10
Sc II	4400.389	0.61	-0.540	syn	1.48	syn	1.00	syn
Sc II	4415.544	0.59	-0.670	syn	1.73	syn	1.48	syn	1.00	syn	1.10
Sc II	5031.010	1.36	-0.400	syn	1.58	syn	0.90
Sc II	5526.785	1.77	0.020	syn	1.68	syn
Sc II	5657.907	1.51	-0.600	no	no	22.67	1.13
Ti I	3904.784	0.90	0.030	68.23	3.61
Ti I	3989.760	0.02	-0.062	102.63	3.89	109.57	3.69
Ti I	3998.640	0.05	0.010	101.96	3.83	109.54	3.65	70.31	2.99
Ti I	4008.928	0.02	-1.016	61.76	3.92	74.65	3.78	32.19	3.03
Ti I	4512.730	0.84	-0.424	47.02	3.85	59.00	3.71
Ti I	4518.020	0.83	-0.269	52.39	3.80	54.06	3.46	29.94	3.10
Ti I	4533.249	0.85	0.532	85.93	3.70	105.24	3.79	70.33	3.07	47.64	2.79
Ti I	4534.780	0.84	0.336	79.03	3.74	80.82	3.42	56.97	3.00	48.81	2.99
Ti I	4535.567	0.83	0.120	83.43	4.06	90.71	3.87	40.54	3.03
Ti I	4544.687	0.82	-0.520	40.86	3.81	59.84	3.81
Ti I	4548.760	0.83	-0.298	49.36	3.77	48.53	3.38	19.71	2.88
Ti I	4555.490	0.85	-0.432	42.51	3.79	49.78	3.55
Ti I	4656.470	0.00	-1.289	42.17	3.72	54.33	3.52	20.98	2.98	15.89	2.94
Ti I	4681.910	0.05	-1.015	62.23	3.87	78.86	3.79	25.48	2.86	24.60	2.96
Ti I	4840.870	0.90	-0.453	46.99	3.93
Ti I	4981.730	0.84	0.560	95.98	3.82	97.31	3.51	58.55	2.94
Ti I	4991.070	0.84	0.436	88.90	3.80	105.73	3.81	59.80	2.92	44.68	2.79
Ti I	4999.500	0.83	0.306	80.76	3.39	39.26	2.67	42.58	2.86
Ti I	5007.206	0.82	0.168	90.09	4.07	92.76	3.78	44.71	3.03
Ti I	5014.187	0.00	-1.220	24.03	3.08
Ti I	5016.160	0.85	-0.518	41.37	3.83
Ti I	5020.024	0.84	-0.358	55.91	3.55
Ti I	5024.843	0.82	-0.546	42.79	3.85	61.21	3.83

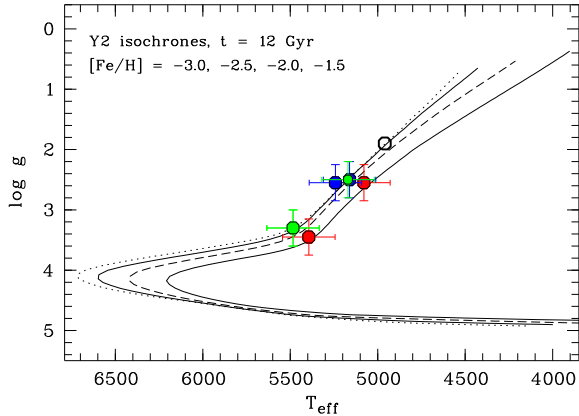


FIG. 2.— Final stellar parameters in comparison with 12 Gyr isochrones with $[\alpha/\text{Fe}] = 0.4$ and metallicity ranging from $[\text{Fe}/\text{H}] = -1.5$ to -3.0 (Green et al. 1984; Kim et al. 2002). Green circles indicate stars with $[\text{Fe}/\text{H}] < -3.0$, blue circles $-3.0 < [\text{Fe}/\text{H}] < -2.0$, red circles $[\text{Fe}/\text{H}] > -2.0$. The black circle shows Segue 1-7 from Norris et al. (2010a).

lower than adopted gravity, but the upper limit of Fe II lines suggest a gravity close to the isochrone or perhaps slightly higher. The spectrum is not consistent with a gravity high enough to place the star on the main sequence. Even with a higher gravity the metallicity does not increase significantly, ruling out the possibility that SDSS J100639+160008 is a more metal-rich foreground star. We furthermore show the spatial distribution of the full sample of Segue 1 members from Simon et al. (2011) in Figure 3, along with the locations of the stars studied in this paper, and also Segue 1-7 from Norris et al. (2010a) which is located near 4 half-light radii, and hence was not covered in the Simon et al. (2011) study.

To investigate the possibility of contamination of the Segue 1 giant sample by foreground stars, we consulted the Besançon model of the Milky Way (Robin et al. 2003). The model predicts that the surface density of Milky Way stars that meet the color and velocity cuts used by Simon et al. (2011) to identify Segue 1 members and have magnitudes consistent with the Segue 1 giants ($19.5 > r > 17$) is $0.8 \text{ stars deg}^{-2}$, or 0.07 stars in the area over which the Simon et al. (2011) survey is essentially complete. This estimate is in agreement with the empirical sample of non-Segue 1 members from Simon et al. (2011). Moreover, $\sim 90\%$ of these potential contaminants are actually on the main sequence, and so would not be confused with Segue 1 giants given the surface gravity measurements from our high-resolution spectra. Thus, we expect only ~ 0.01 Milky Way halo giants with the same color, magnitude, and velocity as Segue 1 to be spatially coincident with the galaxy; since there are only 7 Segue 1 giants, it is very unlikely that our sample contains a Milky Way star masquerading as a Segue 1 member.

4. CHEMICAL ABUNDANCE SIGNATURE OF SEGUE 1

Our abundance analysis was carried out in a standard way, with the goal of producing abundance patterns for our sample stars to characterize the chemical history of Segue 1. The final abundances are presented in Table 6. We also note that we determined abundances for Segue 1-7, for which equivalent widths were published

TABLE 3
STELLAR PARAMETERS

Star	T_{eff} [K]	$\log(g)$ [dex]	$[\text{Fe}/\text{H}]$ [dex]	v_{micr} [km s $^{-1}$]
SDSS J100714+160154	5394	3.45	-1.42	1.70
SDSS J100710+160623	5079	2.55	-1.67	1.75
SDSS J100702+155055	5161	2.50	-2.32	1.80
SDSS J100742+160106	5242	2.55	-2.40	1.70
SDSS J100652+160235	5484	3.30	-3.60	1.35
SDSS J100639+160008	5170	2.50	-3.78	1.55
Segue 1-7	4960	1.90	-3.57	1.30

NOTE. — Segue 1-7 values are taken from Norris et al. (2010a).

by Norris et al. (2010a). The abundances agree within 0.05 dex. For more general details on the element measurements as well as their nucleosynthetic origins, we refer the reader to the discussion in Frebel et al. (2010b), who analyzed spectra of similar metal-poor stars in Ursa Major II and Coma Berenices. However, some details are repeated here for completeness.

4.1. Carbon

Carbon is an important element for tracing early star formation as well as enrichment and nucleosynthesis processes. We measured the carbon abundances in all the stars from two CH features at $\sim 4313 \text{ \AA}$ and 4323 \AA . SDSS J100710+160623, SDSS J100702+155055 and SDSS J100742+160106 (with $[\text{Fe}/\text{H}] = -1.7, -2.3$ and -2.4 , respectively) have $[\text{C}/\text{Fe}]$ abundances close to the solar ratio. This is typical for many metal-poor stars, as can be seen in Figure 4. On the contrary, SDSS J100714+160154 is found to possess a very large overabundance of carbon. Given another critical abundance clue – enhanced neutron-capture element abundances associated with the s-process (see below) – this star appears to be a mildly metal-poor CH star that received its carbon from a binary companion.

At $[\text{Fe}/\text{H}] = -3.6$ and -3.7 , SDSS J100652+160235 and SDSS J100639+160008 have large $[\text{C}/\text{Fe}]$ values of 0.9 and 1.2, respectively. Together with Segue 1-7, having $[\text{C}/\text{Fe}] = 2.3$ at $[\text{Fe}/\text{H}] = -3.6$, they can be classified as carbon-enhanced metal-poor (CEMP) stars, as their carbon exceeds a threshold value of $[\text{C}/\text{Fe}] = 0.7$ (Aoki et al. 2007). With the three most metal-poor stars in Segue 1 being CEMP stars, and keeping in mind that our Segue 1 sample is small, $\sim 50\%$ of Segue 1’s brightest stars presumably formed from gas that was enriched in carbon. (Here we are excluding SDSS J100714+160154 since its carbon abundance is an obvious result of a mass transfer event.) Moreover, this also implies that the CEMP fraction is $\gtrsim 50\%$ for stars with $[\text{Fe}/\text{H}] < -3.5$.

The fraction of CEMP stars among metal-poor halo stars is known to increase with decreasing metallicity (e.g., Rossi et al. 1999; Frebel et al. 2006a; Lucatello et al. 2006; Cohen et al. 2006), pointing to the importance of carbon in the early Universe. Beginning with 15% of stars with $[\text{Fe}/\text{H}] < -2.0$ and 18% at $[\text{Fe}/\text{H}] < -2.5$, the fraction becomes 25% among stars with $[\text{Fe}/\text{H}] < -3.0$, 45% at $[\text{Fe}/\text{H}] \leq -3.5$ and 100% below $[\text{Fe}/\text{H}] < -5.0$ (based on literature data collected by Frebel 2010). A new study by Lee et al. (2013b) based on hundreds of thousands of SDSS stars with

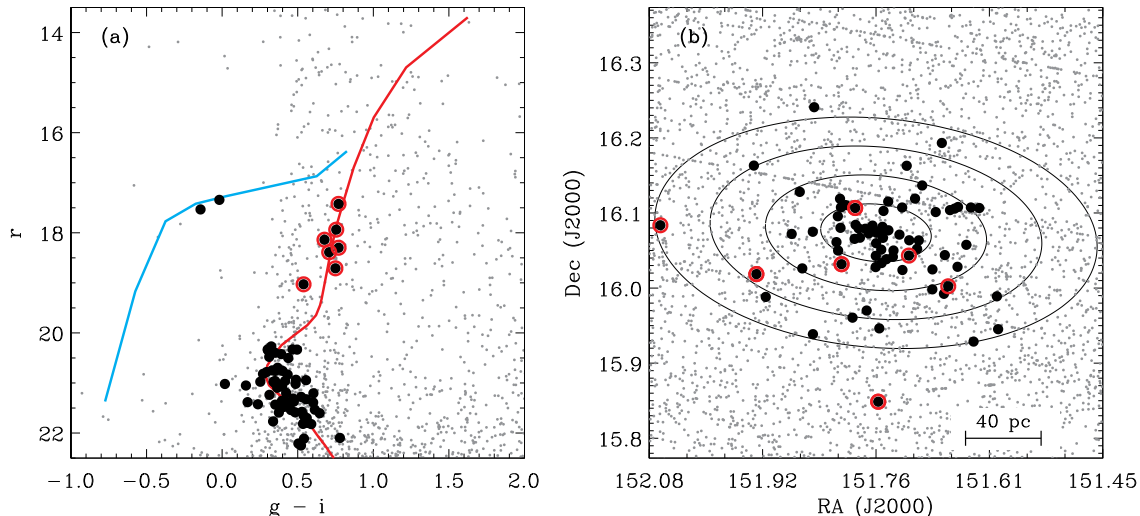


FIG. 3.— Color-magnitude diagram of Segue 1 (left panel) together with the spatial distribution of the stars (right panel). In the left panel, the black points are the 71 Segue 1 members identified by Simon et al. (2011) plus Segue 1-7 from Norris et al. (2010a). The stars outlined in red are the 7 giants discussed in this paper, and the gray dots are all stars from the SDSS catalog in the area shown in the right panel. The RGB/main sequence fiducial track is the slightly modified M92 sequence from Simon et al. (2011; originally taken from Clem et al. 2008), and the HB track is from M13. The symbols are the same in the right panel, and ellipses marking 1, 2, 3, and 4 half-light radii are overplotted.

medium-resolution spectra finds similar results. The CEMP fraction for red giants in the halo is $31\% \pm 4\%$ at $[\text{Fe}/\text{H}] \leq -3.0$ and $33\% \pm 11\%$ at $[\text{Fe}/\text{H}] \leq -3.5$. The Segue 1 measurements suggest that the tendency of the most metal-poor stars to show carbon enhancement is not limited to the halo, but may also be a general feature of dwarf galaxies.

A possible explanation for this early presence of large amounts of carbon could be the existence of rotating massive stars. They could have provided large amounts of CNO elements during their evolution and/or supernova explosion (e.g., Meynet et al. 2006). Moreover, low-mass star formation may be facilitated in carbon-rich environments because carbon (together with oxygen⁹) may have provided a cooling channel for the primordial gas to sufficiently fragment (Bromm & Loeb 2003; Frebel et al. 2007a). If so, the carbon abundance of the entire system would need to be above the critical metallicity for the observed stars to have formed. Indeed, $[\text{C}/\text{H}] > -3.0$ for all stars, which is well above $D_{\text{trans}} = \log(10^{[\text{C}/\text{H}]} + 0.9 \times 10^{[\text{O}/\text{H}]}) > -3.5$ (Frebel et al. 2007a).

An alternative explanation for the carbon-enhancement would be mass transfer from an unseen intermediate mass binary companion that went through the AGB phase. However, at least those carbon-enhanced metal-poor stars that have been shown to be in binary systems also show significant amounts of s-process material and only occur at metallicities of $[\text{Fe}/\text{H}] \gtrsim -3.0$ (e.g. Masseron et al. 2010). The three carbon-enhanced EMP stars in Segue 1 are different (i.e. they can be classified as CEMP-no stars) and have $[\text{Fe}/\text{H}] < -3.5$. For those stars, the binary fraction is currently unknown (Masseron et al. 2010). Future radial velocity monitoring of CEMP stars will reveal whether the binary scenario could explain carbon-enhancement

at $[\text{Fe}/\text{H}] < -3.5$.

Following Frebel & Bromm (2012), an early galaxy should show large abundance spreads in terms of $[\text{X}/\text{H}]$, as a result of inhomogeneous mixing of supernova metal yields (e.g., Greif et al. 2011). For $[\text{Fe}/\text{H}]$, Segue 1 shows a > 2 dex spread. For $[\text{C}/\text{H}]$ this is also nearly 2 dex (again, excluding SDSS J100714+160154). The stars with higher $[\text{Fe}/\text{H}]$, however, are not CEMP stars by the current definition because their high $[\text{Fe}/\text{H}]$ keeps the $[\text{C}/\text{Fe}]$ ratio down. In considering this criterion for an entire galaxy it also becomes clear that the definition for stellar carbon enhancement, being based on the $[\text{C}/\text{Fe}]$ ratio, may be an insufficient description. Regardless, assuming inhomogeneous mixing throughout Segue 1 resulting in $[\text{X}/\text{H}]$ spreads, and keeping in mind that the carbon enrichment processes were likely completely different and/or decoupled from that of iron, the important conclusion is that all stars show a $[\text{C}/\text{H}]$ abundance in excess of the critical amount, independent of their $[\text{Fe}/\text{H}]$. Coming back to the large fraction of CEMP stars observed in the halo, it is plausible that the halo CEMP stars (and some more metal-rich stars, although they would be very difficult to identify) formed in environments similar to that of Segue 1.

4.2. α -elements

Abundances of the α -elements magnesium, calcium and titanium were obtained from equivalent width measurements. We used spectrum synthesis to determine the silicon abundance. All four α -element abundances are enhanced at the $[\alpha/\text{Fe}] \sim 0.5$ dex level, even in the more metal-rich stars including SDSS J100714+160154. Figure 5 shows the abundance trends of all four α -elements, in comparison with various halo and dwarf galaxy stars. In Figure 6 we also show the comparison of all our elemental abundances specifically with those of the extremely metal-poor star sample from Cayrel et al. (2004). Generally, the agreement between the samples is

⁹ Oxygen and nitrogen features were not detected in our spectra.

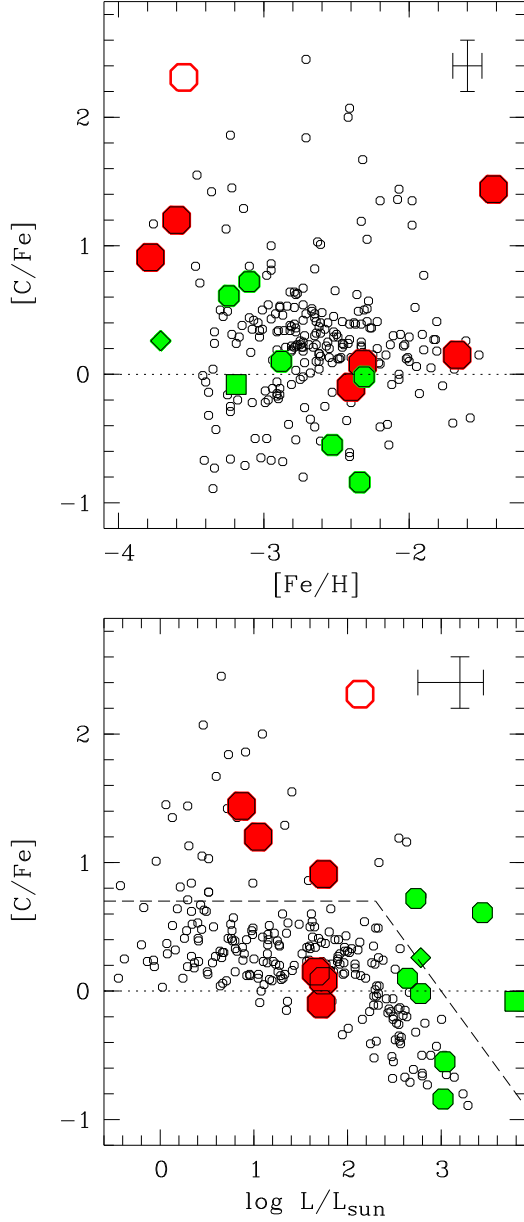


FIG. 4.— $[C/Fe]$ abundance ratios (filled red circles) as a function of $[Fe/H]$ (top panel) and stellar luminosity (bottom panel), in comparison with metal-poor halo stars from Barklem et al. (2005). The definition of C-enhancement from Aoki et al. (2007) is shown with a dashed line. Representative error bars are also shown. The three most metal-poor stars (including Segue 1-7 of Norris et al. 2010a, open red circle) are carbon-enhanced. The more metal-rich stars have carbon abundances near the solar ratio (dotted line), with the exception of the CH star SDSS J100714+160154. Green smaller circles are stars in UMaII, ComBer (Frebel et al. 2010b) and Leo IV (Simon et al. 2010).

excellent.

Despite the broad agreement between the abundance patterns in Segue 1 and halo stars, careful examination of Fig. 5 reveals that the Segue 1 stars have ~ 0.1 dex higher abundances in each of the α -elements. However, this could be due to differences in surface gravity, $\log g_f$ values and stellar parameter determinations. Similar behavior was found by Hollek et al. (2011), who traced higher Mg abundances to using systematically

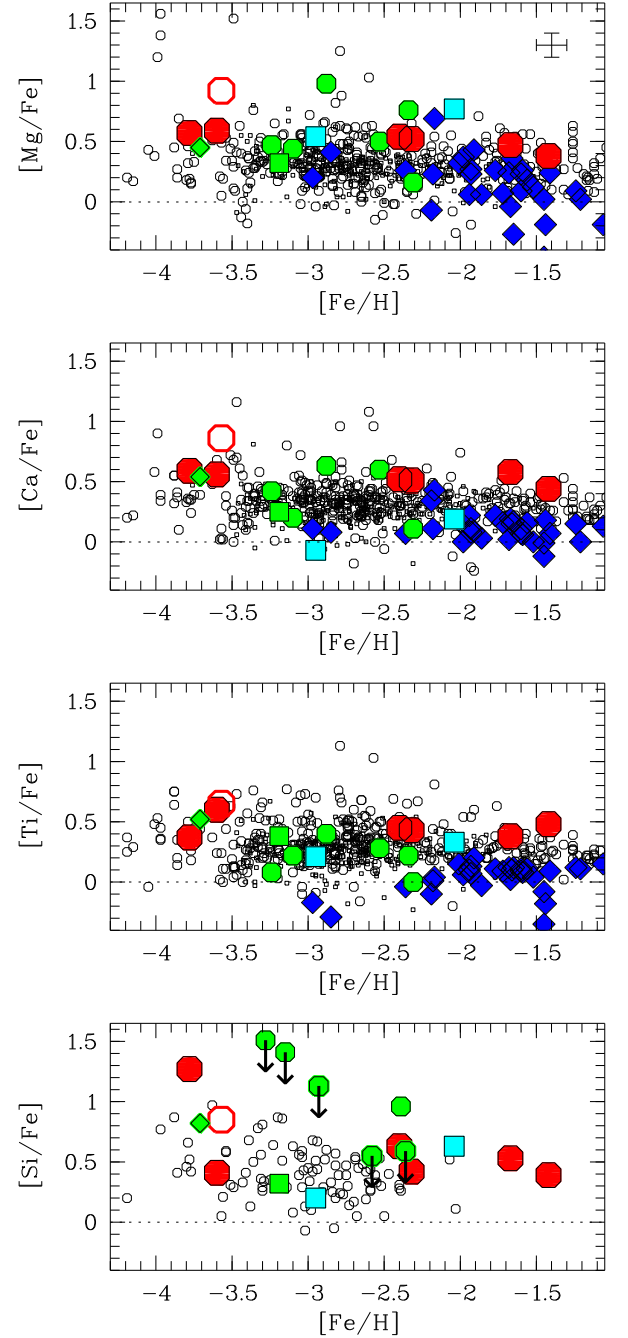


FIG. 5.— Abundance ratios of α -elements $[Mg/Fe]$, $[Ca/Fe]$, $[Ti/Fe]$ and $[Si/Fe]$ in our Segue 1 stars (filled red circles) and star Segue 1-7 from Norris et al. (2010a) (open red circle) in comparison with those of other ultra-faint dwarf galaxy stars (UMaII, ComBer, Leo IV; green circles (Frebel et al. 2010b; Simon et al. 2010); Boötes I; green diamond; (Norris et al. 2010c); Hercules and Draco; cyan squares (Koch et al. 2008; Fulbright et al. 2004)), stars in the classical dwarfs (blue triangles; Venn et al. 2004), and Galactic halo stars (black open circles; Cayrel et al. 2004; Venn et al. 2004; Aoki et al. 2005; Barklem et al. 2005; Yong et al. 2013). For Si, much less data is available. A representative error bars is shown in the $[Ca/Fe]$ panel.

lower gravities than other studies. We tested this possibility by independently deriving abundances for five stars in the Cayrel et al. sample (HD2796, HD122563, BD -18 deg 5550, CS22892-052, CS31082-001), using their

published equivalent widths and our $\log gf$ values and methods of determining stellar parameters. A stellar parameter comparison between studies can be found in (Frebel et al. 2013a). We find that using our technique produces no significant differences between our Segue 1 $\log \epsilon(X)$ abundances and the respective published Cayrel et al. abundances. The mean difference between the two studies for each element (O, Na, Mg, Al, Si, Ca, Sc, Ti I, Ti II, Cr, Mn, Fe I, Fe II, Co, Ni, Zn) ranges from ~ 0.00 to ~ 0.1 dex with respective standard errors of the mean about as large or larger than the mean values. There are only two exceptions where the differences are more significant; there is an abundance difference for Na of 0.19 ± 0.04 and 0.11 ± 0.015 for Mg. Indeed, our Mg abundance are systematically higher by 0.1 dex owing to slightly lower surface gravities. The other α -elements Si, Ca and Ti, however, are not gravity sensitive and yield essentially identical abundances. Given the good agreement with the Cayrel et al. stars we conclude that the Segue 1 α -elements show the same behavior as what is found in typical metal-poor halo stars with $[\text{Fe}/\text{H}] \lesssim -1.5$, which is consistent with massive stars having enriched Segue 1 at the earliest times.

Another noteworthy issue is that the EMP star Segue 1-7 has somewhat higher abundance ratios than the other Segue 1 stars. Our re-analysis of the published equivalent widths from Norris et al. (2010a) yielded slightly lower values, but Segue 1-7 remains with marginally enhanced α -abundances relative to both the halo sample and the rest of Segue 1. We also find that two of the three Segue 1 EMP stars, SDSS J100639+160008 and Segue 1-7, show an enhancement in silicon of $[\text{Si}/\text{Fe}] = 1.2$ and 0.8 , respectively, which is well above the halo-typical α -enhancement. The SDSS J100639+160008 Si abundance was derived from the line at 3905 \AA , which is nearly saturated. The line is known to be blended with a CH feature, but given the strength of the line, the contribution of CH to the observed absorption is a minor issue. The Si abundance of Segue 1-7 is based on the 4102 \AA line (Norris et al. 2010a) and somewhat uncertain. The similarly high Ca and Mg abundances of this star lend support to the Si measurement.

Interestingly, though, there are other metal-poor halo stars with $[\text{Fe}/\text{H}] < -2.5$ that exhibit similar behavior to these two stars. We find 12 stars in the Frebel (2010) database of metal-poor stars that have $[\text{Si}/\text{Fe}] > 0.6$ and $[\text{Si}/\text{Mg}] > 0.4$ (four stars from Cayrel et al. 2004, two stars each from McWilliam et al. 1995, Aoki et al. 2002b and Lai et al. 2008, and one star each from Preston et al. 2006 and Frebel et al. 2007b). We use the $[\text{Si}/\text{Mg}]$ ratio to select stars that are not enhanced both in Si and Mg, as those exist as well. In addition to these 12 stars, S1020549, a star with $[\text{Fe}/\text{H}] = -3.8$ in Sculptor (Frebel et al. 2010a) and one in Ursa Major II (Frebel et al. 2010b) also show Si abundances of $[\text{Si}/\text{Fe}] \sim 1.0$ (although the Ursa Major II star also has $[\text{Mg}/\text{Fe}] \sim 0.7$).

These results demonstrate that high Si abundances (with and without significant Mg overabundances) are a rather ubiquitous feature indicating massive star enrichment driven by supernova explosions that are perhaps sensitive to progenitor properties (Aoki et al. 2002a). In-

deed, Si is made in both hydrostatic and explosive oxygen burning processes. A different fraction of the Si produced during stellar evolution may survive to the SN explosion (Woosley & Weaver 1995) depending on the stellar mass as well as on the uncertain values for the $^{12}\text{C}(\alpha, \gamma)^{16}\text{O}$ reaction rate. Hence, this could explain the relatively large spread in the observed abundances as simply resulting from different stellar progenitor properties.

Considering all of the Segue 1 stars, what appears most striking is that overall, the $[\alpha/\text{Fe}]$ ratios are all enhanced and nearly identical. Moreover, there is no evolution evident with metallicity, even above $[\text{Fe}/\text{H}] > -2$. The same behavior was found by Vargas et al. (2013), who used medium-resolution spectra to determine α -abundances for stars in many ultra-faint dwarf galaxies, including Segue 1. The absence of a decline in $[\alpha/\text{Fe}]$ with $[\text{Fe}/\text{H}]$ indicates no significant contribution of Fe by Type Ia supernovae to the gas clouds from which the observed stars formed. Instead, the evidence suggests that Segue 1 was enriched by massive stars alone. It is particularly notable that the highest metallicity star in the galaxy (with $[\text{Fe}/\text{H}] = -1.4$) has an average $[\alpha/\text{Fe}] = 0.43$, consistent with massive star enrichment. For comparison, this halo-like, massive-progenitor-star α -enhancement is not found among metal-poor stars with $-2.5 \lesssim [\text{Fe}/\text{H}] \lesssim -1.5$ in the classical dwarf galaxies. Those stars show lower $[\alpha/\text{Fe}]$ values close to the solar value, indicating a slower enrichment timescale of their respective hosts and a chemically “earlier” contribution (i.e., at lower metallicity of the system) of iron by Type Ia supernovae. We therefore conclude that chemical evolution in Segue 1 proceeded differently, or was truncated, in Segue 1 compared to both the classical dwarf spheroidals and most other ultra-faint dwarfs.

4.3. Sodium to zinc

Various abundances of other lighter and iron-peak elements were also determined for our Segue 1 stars. Overall, there is very good agreement with the respective abundances of halo stars of similar metallicities, as can be seen in Figure 6. Below we briefly comment on each element.

The abundances derived from the Na D lines are known to be significantly different in a non-LTE analysis, resulting in large abundance corrections of 0.5 dex for giants (Baumüller et al. 1998). We note that we have not corrected our abundances since the literature abundances are all in LTE, and because our main focus is on an abundance comparison between star samples rather than absolute values. The sodium abundance ratios in our Segue 1 stars are about that of the Sun, within ± 0.3 dex. However, Segue 1-7 has an even higher abundance, increasing the range from $[\text{Na}/\text{Fe}] = 0.54$ dex to 0.87 dex. In halo stars, aluminum is often deficient by almost 1 dex with respect to iron and the Sun. Our stars are no exception, with a small scatter of $[\text{Al}/\text{Fe}] = 0.3$ dex. But as with Na, Segue 1-7’s abundance is unusually high, although some halo stars have similar abundances.

A $[\text{Na}/\text{Fe}]$ spread larger than that of the $[\text{Na}/\text{Al}]$ ratio might be a sign of AGB nucleosynthesis and associated chemical enrichment as is found in globular clusters. We thus discuss Na and Al together to assess this possibility. Not considering Segue 1-7, the spread of $[\text{Na}/\text{Fe}]$ and $[\text{Na}/\text{Al}]$ are both about 0.5 dex, which is typical for

halo stars. When including Segue 1-7, the $[\text{Al}/\text{Fe}]$ spread does indeed become ~ 0.2 dex larger than the $[\text{Na}/\text{Fe}]$ spread. However, globular clusters typically have high Al abundances of $[\text{Al}/\text{Fe}] > 0.4$ (e.g., Yong et al. 2005; Carretta et al. 2012). None of the seven Segue 1 stars shares this trait. An enrichment similar to what is occurring within globular clusters can thus be ruled out. Instead, the signature of Segue 1-7 of high C, Na, Mg, and Al abundances – a pattern that has been found for some other metal-poor halo stars also (Aoki et al. 2002a) – perhaps rather signals a particular kind of supernova explosion as the source of early metals in Segue 1.

Scandium abundances show a tight trend in halo stars, and all Segue 1 abundances agree extremely well with them. Chromium, manganese, cobalt and nickel are all very similar in this regard, and again there is excellent agreement of all Segue 1 abundances with the respective halo ratios. Since Mn was difficult to obtain for SDSS J100652+160235, we can only present an upper limit. Segue 1-7 has an unusually low Ni abundance. However, it was only determined from one line (Norris et al. 2010a). Finally, for completeness, we note that a zinc abundance could only be determined for the most metal-rich Segue 1 star. We show upper limits in Figure 6 for all other stars.

4.4. Neutron-capture elements

An emerging abundance characteristic of stars in the ultra-faint dwarf galaxies that have been observed at high spectral resolution is that they all display extremely low levels ($[\text{n-cap}/\text{Fe}] \ll 0.0$) of neutron-capture elements (e.g., Koch et al. 2008; Frebel et al. 2010b; Simon et al. 2010; Norris et al. 2010a,c; François et al. 2012; Koch et al. 2013). Segue 1 is no exception, having the lowest overall neutron-capture abundance level of any known system.

We attempted to measure abundances from the Sr II line at 4077 Å and the Ba II line at 4554 Å. There is a weak Ba detection in SDSS J100742+160106 and clearly visible Sr and Ba lines in SDSS J100714+160154 (which is the most metal-rich star and discussed separately below). Segue 1-7 also has a Sr detection (Norris et al. 2010a). For all other stars we could only derive upper limits on these two elements. Portions of the spectra around the Ba line can be seen in Figure 1 (left panel). This line is generally easily detected in metal-poor stars, even in noisy spectra, and especially in the stars with $[\text{Fe}/\text{H}] > -2.5$. Hence, it is rather unusual that it is not detected in most stars in Segue 1. For example, SDSS J100710+160623 has very low upper limits of $[\text{Sr}/\text{Fe}] < -3.2$ and $[\text{Ba}/\text{Fe}] < -2.6$. These are the lowest $[\text{Sr}/\text{Fe}]$ and $[\text{Ba}/\text{Fe}]$ values ever determined (see top panels in Figure 8). However, when normalizing to hydrogen rather than iron to assess the overall level of enrichment in Segue 1, the upper limits of SDSS J100710+160623 are at the same level as those of the other stars (bottom panel in Figure 8), $[\text{Sr}/\text{H}] \lesssim -5$ and $[\text{Ba}/\text{H}] \lesssim -4.4$.

More specific clues regarding the level at which neutron-capture elements are present in this galaxy come from Segue 1-7 (Norris et al. 2010a) which has a measured Sr abundance of $[\text{Sr}/\text{H}] = -4.9$, and from SDSS J100742+160106 which has a weak Ba measurement of $[\text{Ba}/\text{H}] = -4.5$. However, the Ba line in Segue 1-7 is not detected, resulting in a limit of $[\text{Ba}/\text{H}] < -4.5$.

Similarly, SDSS J100742+160106 has an upper limit for Sr of $[\text{Sr}/\text{H}] < -5.2$. The two detections, together with the upper limits of the other stars confirm that Segue 1, as a system, is extremely deficient in neutron-capture elements, at or below the 10^{-5} level in $[\text{Sr}/\text{H}]$ and $10^{-4.5}$ level in $[\text{Ba}/\text{H}]$. Nevertheless, it is apparent from the handful of Sr and Ba detections that there is neutron-capture material present in Segue 1, as is the case in every other known stellar system (Roederer 2013).

In Figure 8, the yellow shaded area indicates the upper enrichment level of Sr, bounded by Segue 1-7 at the high end. The same is shown for $[\text{Ba}/\text{H}]$ with the measurement of SDSS J100742+160106 as the upper bound. It is interesting to note, though, that a handful of EMP halo stars have Sr and Ba abundances that are up to 1 dex lower than our upper enrichment bounds, showing that detections of these elements at the $[\text{Sr}/\text{H}] \sim -6$ or $[\text{Ba}/\text{H}] \sim -5.5$ level are possible, likely owing to much higher data quality. No halo stars above $[\text{Fe}/\text{H}] = -2.5$ that are so deficient in the heaviest elements have yet been identified, demonstrating that systems like the ultra-faint dwarfs cannot have contributed appreciably to the halo in this metallicity range (see § 5).

According to Simon et al. (2011), Segue 1 has a mass within its half light radius of $\sim 6 \times 10^5 M_\odot$. Its stellar mass, however, is only $\sim 10^3 M_\odot$ (Martin et al. 2008). Since a typical star formation efficiency is 1% per free fall time (Krumholz & Tan 2007), even if star formation in Segue 1 only lasted for a single free fall time, the initial gas cloud out of which the Segue 1 stars formed was likely $\sim 10^5 M_\odot$. Larger gas masses would exceed the cosmic baryon fraction at the center of Segue 1, although if one considers the halo mass of the galaxy larger amounts of baryons could be allowed. Assuming that the gas comprising Segue 1 was (instantaneously and homogeneously) enriched by a first supernova at the earliest times, an average abundance of $[\text{Sr}/\text{H}] = -5.0$ (roughly that of Segue 1-7) would imply a total Sr mass of only $\sim 10^{-7} M_\odot$. However, the average Sr abundance was likely less than that of Segue 1-7 (as indicated by our lowest upper limit of $[\text{Sr}/\text{H}] > -5.2$), which would decrease the required total Sr mass present at Segue 1 at early times. Hence, we regard $\sim 10^{-7} M_\odot$ of Sr as a reasonable estimate. In the same way, less than $\sim 10^{-7} M_\odot$ of Ba appears to be present in Segue 1, assuming $[\text{Ba}/\text{H}] < -4.5$.

These extremely small amounts of neutron-capture elements could have come from just a single neutron-capture element production event. Possibilities include the r-process occurring in a core-collapse supernova, yielding of order $10^{-4} M_\odot$ of neutron-capture elements (Farouqi et al. 2010) or the s-process that may have operated in a massive rotating star, perhaps a Population III star (e.g., Chiappini et al. 2011; Pignatari et al. 2008, and see Jacobson & Frebel 2013 for a review on neutron-capture element sources). An AGB enrichment event is unlikely as a source for this small amount of neutron-capture material. Models of AGB nucleosynthesis generally suggest much larger amounts to be produced (Karakas 2010; Lugaro et al. 2012). For example, the low-metallicity stellar model described in Placco et al. (2013) loses $0.5 M_\odot$ during its AGB phase. This is orders of magnitude more than what is implied by the observed

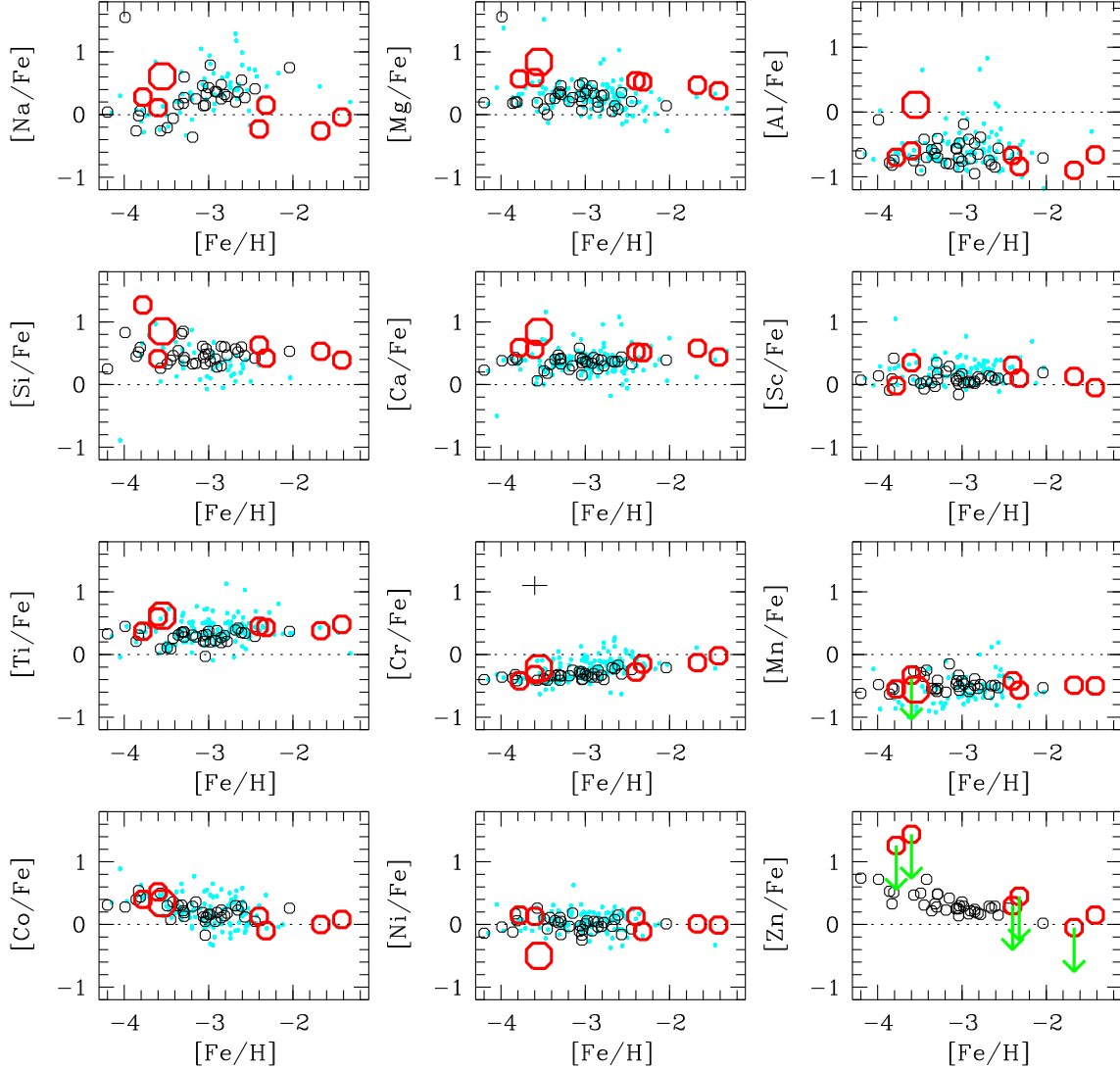


FIG. 6.— Abundance ratios ($[X/Fe]$) as a function of metallicity ($[Fe/H]$) for various elements detected in our Segue 1 stars (small open red circles) and star Segue 1-7 from Norris et al. (2010a) (large red open circle) in comparison with those of halo stars (black circles) of Cayrel et al. (2004) and Yong et al. (2013) (small blue points).

low Sr and Ba abundances in the Segue 1 stars.

More detailed yield calculations, paired with simulations of metal-mixing in such small systems, are required to fully characterize the neutron-capture enrichment process in systems like Segue 1. However, the fact that Segue 1 has such a uniformly low overall neutron-capture abundance suggests that the halo stars with equally low $[Sr/H]$ and $[Ba/H]$ may have originated in similar systems before being accreted by the Milky Way.

To complete the discussion on the neutron-capture elements, we also have to revisit SDSS J100714+160154. At $[Fe/H] = -1.4$ it has $[Sr/Fe] = +0.90$ and $[Ba/Fe] = +1.85$. These high values are difficult to reconcile with those of the other Segue 1 stars unless SDSS J100714+160154 has a different enrichment history. We suggest that SDSS J100714+160154 is likely a CH star in a binary system that underwent mass transfer. General CH star characteristics are moderate metallicity around $[Fe/H] \sim -1.5$, high carbon abundance in combination with s-process enrich-

ment, and radial velocity variation. The radial velocity measured from our MIKE spectrum agrees within the uncertainties with those determined by Simon et al. (2011), so binary amplitudes larger than $\sim 10 \text{ km s}^{-1}$ are unlikely. Despite the lack of evidence for binary orbital motion, SDSS J100714+160154 does have $[Fe/H] \sim -1.4$, $[C/Fe] = 1.4$, and also $[Pb/Fe] \sim 2.0$. High lead abundances are a signature of the s-process, and together with the overabundance in carbon, SDSS J100714+160154's abundance pattern is clearly consistent with that of a CH star. In Figure 7 we show the few measurable neutron-capture element abundances in SDSS J100714+160154 compared to the solar r- and s-process patterns (Burris et al. 2000). While the number of neutron-capture element abundance is limited, the pattern matches that of the solar s-process. Hence, the star's neutron-capture material is not a reflection of the birth gas cloud composition but is due to a later-time external enrichment event following mass transfer from the binary companion. While our sample is too small for a

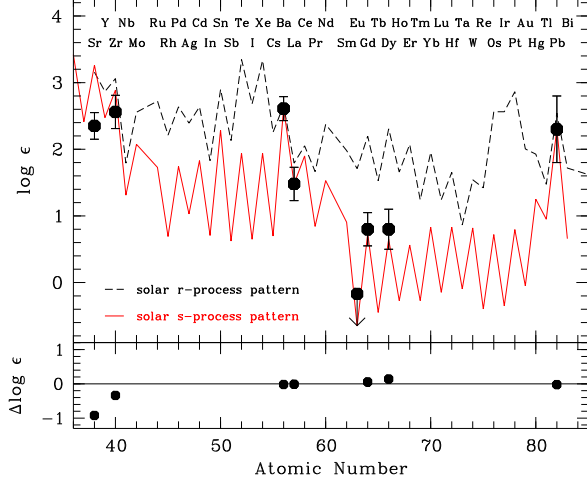


FIG. 7.— Neutron-capture element abundances in SDSS J100714+160154 compared to the solar r- and s-process patterns (Burris et al. 2000). SDSS J100714+160154 clearly shows a signature of the s-process.

statistical analysis and also lacks long-term radial velocity monitoring, finding one binary in a sample of seven stars suggests that the binary fraction is substantial, consistent with the results of Martinez et al. (2011). Binary stars, and thus mass transfer events, are very common in general, so it is perhaps not too surprising that a star in our sample shows these characteristics.

4.5. Abundance uncertainties

Given that we use our abundances to constrain a number of processes related to early star formation, chemical enrichment and metal mixing, it is important to carefully consider any abundance uncertainties. Using a formula in Frebel et al. (2006b) to estimate the uncertainties on our equivalent width measurements (taking into account the S/N of the spectrum, pixel width and number of pixels across a spectral line), we estimate our measurements to have 3σ uncertainties of 10 to 15%. This corresponds to up to 0.15 to 0.2 dex (and in the case of SDSS J100742+160106 to up to ~ 0.3 dex) changes in abundances. These uncertainties are reflected in the standard deviations of our line abundances for each element (see Table 2) which range from 0.10 to 0.25 dex, and are listed in Table 4. We also derived systematic uncertainties of our abundances for two example stars by changing one stellar parameter at a time by an amount approximately equal to its random uncertainty. Uncertainties from different sources of random errors (std. dev. of the line abundances for a given element), systematic errors, and the total uncertainty for each element are given in Table 4. Overall, typical total uncertainties range from 0.15 to 0.30 dex.

Many abundances are based on only a few lines so that the associated standard errors are unrealistically small (< 0.05 dex) compared with typical measurement uncertainties. We thus adopt a minimum uncertainty of 0.10 dex in such cases. Furthermore, for abundances of elements derived from only one line, we adopt a formal uncertainty of 0.15 dex, which should reasonably reflect our largest source of error, continuum placement uncertainties. Despite having two measurements for C,

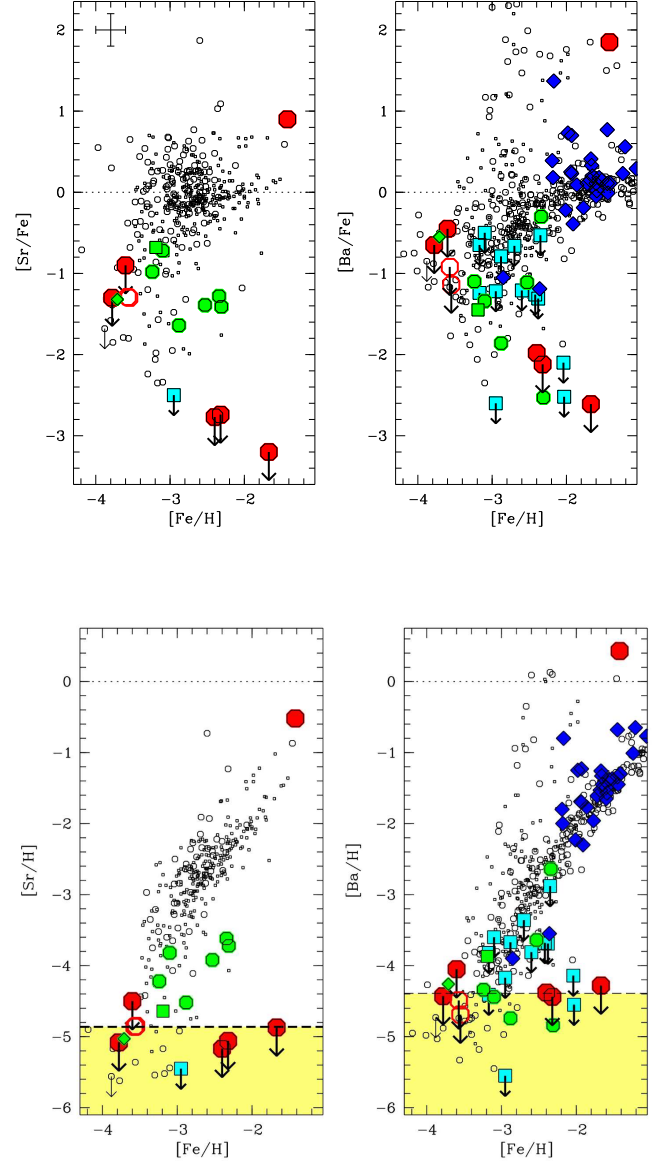


FIG. 8.— Abundance ratios of neutron-capture-elements $[Sr/Fe]$ and $[Ba/Fe]$ (top panel) and $[Sr/H]$ and $[Ba/H]$ (bottom panel) as a function of metallicity $[Fe/H]$ of our Segue 1 stars (filled red circles) and star Segue 1-7 (open red circle; Norris et al. 2010a) in comparison with those of other ultra faint dwarf galaxy stars in UMa II, ComBer, Leo IV (green circles; Frebel et al. 2010b; Simon et al. 2010), Draco and Hercules (cyan squares; Fulbright et al. 2004; Koch et al. 2008, 2013), stars in the classical dwarfs (blue triangles; Venn et al. 2004), and the galactic halo (black open circles; Aoki et al. 2005, François et al. 2007, Barklem et al. 2005 and Yong et al. 2013). Note that both axes have the same scale, showing the huge range of neutron-capture abundances in metal-poor stars. A representative error bars is shown in the $[Sr/H]$ panel.

we adopt 0.20 dex for this element since the continuum placement was difficult for spectral regions with molecular bands. Finally, uncertainties on iron abundances are also somewhat larger. This is due to our method of correcting the spectroscopic temperatures, which introduces a slope of line abundance as a function of excitation po-

TABLE 4
EXAMPLE ABUNDANCE UNCERTAINTIES FOR
SDSS J100710+160623 AND SDSS J100652+160235

Element	Standard deviation	ΔT_{eff} +100 K	$\Delta \log g$ +0.3 dex	Δv_{micr} +0.3 km s ⁻¹	Total ^a Unc.
SDSS J100710+160623					
C (CH)	0.20	0.02	-0.03	0.12	0.24
Na I	0.10	0.14	-0.12	-0.10	0.23
Mg I	0.10	0.10	-0.10	-0.08	0.19
Al I	0.25	0.14	-0.13	-0.11	0.33
Si I	0.15	0.07	-0.01	-0.06	0.18
Ca I	0.23	0.09	-0.09	-0.12	0.29
Sc II	0.12	0.02	0.10	-0.09	0.18
Ti I	0.15	0.15	-0.04	-0.12	0.25
Ti II	0.15	0.02	0.09	-0.12	0.21
Cr I	0.16	0.13	-0.02	-0.08	0.22
Cr II	0.15	-0.04	0.10	-0.03	0.19
Mn I	0.15	0.14	-0.05	-0.13	0.25
Fe I	0.22	0.12	-0.04	-0.12	0.28
Fe II	0.18	0.03	0.10	-0.08	0.22
Co II	0.07	0.17	-0.02	-0.18	0.26
Ni I	0.16	0.10	-0.01	-0.06	0.20
SDSS J100652+160235					
C (CH)	0.20	0.08	-0.05	0.12	0.25
Na I	0.10	0.10	-0.03	-0.04	0.15
Mg I	0.06	0.11	-0.09	-0.04	0.16
Al I	0.20	0.08	-0.01	-0.03	0.21
Si I	0.15	0.13	-0.11	-0.10	0.25
Ca I	0.13	0.09	-0.05	-0.05	0.15
Sc II	0.15	0.08	0.08	-0.10	0.21
Ti II	0.14	0.06	0.09	-0.05	0.18
Cr I	0.15	0.09	-0.01	-0.02	0.18
Fe I	0.23	0.13	-0.05	-0.12	0.30
Co II	0.10	0.09	0.00	-0.02	0.14
Ni I	0.15	0.14	-0.05	-0.15	0.26

^a Obtained by adding all uncertainties in quadrature.

tential and thus inflates the standard deviation.

5. ON THE ORIGIN AND EVOLUTION OF SEGUE 1

We now discuss the main chemical abundance signatures to further characterize the nature of Segue 1. Specifically, we aim at testing whether Segue 1 is a surviving first galaxy. If so, Segue 1 could be a surviving member of a population of the earliest building blocks that were available for galaxy formation in the early Universe. We also use Segue 1 to learn about the origin of the most metal-poor stars, assuming that the (outer) Milky Way halo assembled from smaller galaxies over time.

Iron abundance spread: consequences of inhomogeneous mixing of earliest metals Segue 1 contains stars that span a large range in metallicity of more than 2 dex, from $[\text{Fe}/\text{H}] = -1.4$ to $[\text{Fe}/\text{H}] = -3.8$. Given the paucity of observable stars as well as this large Fe spread, the metallicity distribution function – insofar as this term can be applied here – appears to be rather flat. If the true metallicity distribution is roughly Gaussian (e.g., Kirby et al. 2011b), the dispersion must be very large (~ 1 dex). However, if the distribution reflects inhomogeneous mixing at early times rather than steady evolution (see below), then a Gaussian form may not be expected.

According to hydrodynamical simulations by Greif et al. (2011), who studied metal enrichment in a first galaxy, large abundance spreads of several dex in $[\text{X}/\text{H}]$ are found already after the explosion of just one energetic supernova. The Fe spread in the simulations, averaging around $[\text{Fe}/\text{H}] \sim -3$, agrees very well with

what we observe in Segue 1. Furthermore, one important consequence arises from this: in an early galaxy that has only undergone an initial chemical enrichment event but no chemical *evolution* yet, the iron abundance of the stars does not (yet) provide the kind of time sequence that iron usually does in other galaxies, including the more luminous classical dwarf galaxies.

Ordinarily, as star formation and chemical enrichment proceed in a system, increasing numbers of stars with progressively higher metallicities are formed. These stars then build up the familiar metallicity distribution function (e.g., Kirby et al. 2011b) with large numbers of relatively metal-rich stars and a small metal-poor tail that formed at early times. Hidden in the metal-rich end of the MDF, though, should be a few metal-rich stars that were produced at the earliest times as a consequence of inhomogeneous mixing, but identifying such stars would be difficult underneath the dominant younger population at similar metallicities. (Implications of this scenario are further discussed below in relation to the neutron-capture element abundances.) Consequently, the metal-poor tail of an integrated galaxy MDF consists solely of the few metal-poor stars that formed after the first enrichment event(s) and before the system experienced further enrichment. Rather quickly, the overall galaxy metallicity becomes too high to form additional metal-poor stars, and subsequent generations of stars are added only at the metal-rich end of the distribution. In Segue 1, however, this later enrichment may never have occurred.

This would imply that the most metal-poor Galactic stars are a collection of second (and/or perhaps third) generation stars that were born in various small dwarf galaxies. The nature and similarity of their overall elemental abundance patterns reflects massive star progenitors, albeit with indications for some variety among the individual progenitor stars, as would be expected from stochastically sampling the upper end of the IMF. Given that these small systems likely formed from a small number of minihalos that hosted Pop III stars (not necessarily with the same mass or mass function), slight variations in the abundance ratios can be understood in terms of variations in early Pop III stars and the first galaxy assembly processes.

We note that simulations predict that a fraction of the Milky Way’s stellar halo is likely to have formed in situ, rather than being accreted from smaller galaxies (e.g., Zolotov et al. 2009). The chemical abundance patterns resulting from in situ star formation will differ from those seen in the very different environments of dwarf galaxies (Brusadin et al. 2013), which would alter our expectations for the comparison between dwarf galaxy stars and halo stars. However, because in situ stars are thought to be heavily weighted toward the center of the Milky Way and high metallicities (e.g., Zolotov et al. 2010; Tissera et al. 2012), they probably do not comprise a significant part of the halo samples to which we compare.

Carbon enhancement: massive rotating progenitors seeding the first low-mass stars The three most metal-poor stars in Segue 1 are carbon-enhanced. This presence of significant amounts of carbon above a critical metallicity (Frebel et al. 2007a) likely enabled the formation of the now-observed low-mass stars. Even the more

metal-rich stars have high enough $[C/H]$ values in agreement with cooling by carbon and other metals. Moreover, the $[C/H]$ ratios of all stars do not have a clear trend with $[Fe/H]$, suggesting that the production of these elements and their subsequent mixing is decoupled. If (some of) the massive progenitor stars were rapidly rotating, CNO material would have been released prior to their supernovae, resulting in a carbon-enhancement floor, and hence no strong correlation with the supernova-provided elements such as Fe. Consequently, $[C/Fe]$ shows a correlation with $[Fe/H]$, with the most metal-poor stars being more carbon-rich.

Enhanced α -element abundances: no late-time star formation The α -element abundance ratios indicate what type of stars provided the observed elements. The top panel of Figure 9 schematically depicts the differences between the chemical evolution and enrichment history of various galaxies: the Milky Way halo, the classical dwarfs with slower chemical evolution, and the early systems with essentially no evolution at all. Segue 1 stars all have enhanced $[\alpha/Fe]$ values consistent with chemical enrichment of their birth gas cloud by massive stars, with no contribution from other sources of heavy elements. We show the combined $[\alpha/Fe]$ abundances for the Segue 1 stars in the bottom panel of Figure 9 (red circles). On the other hand, the Milky Way halo (middle panel) was enriched rapidly to $[Fe/H] \approx -1$ by core-collapse supernovae before Type Ia supernovae began to add significant amounts of iron. In the classical dSphs (lower panel, black circles), the Type Ia contribution (which is assumed to occur after a similar delay time in all galaxies) is visible at lower metallicities, $-2.5 \lesssim [Fe/H] \lesssim -1.5$ (Venn et al. 2004; Letarte et al. 2010; Kirby et al. 2011a; Lemasle et al. 2012), indicating that less enrichment took place during the pre-Ia epoch.

The fact that Segue 1 shows enhanced $[\alpha/Fe]$ abundances for all metallicities reflects rapid and inhomogeneous metal mixing, consistent with the predictions of Frebel & Bromm (2012) for the chemical signature of a first or very early galaxy: the observed stars should show no sign of AGB star or supernova Ia enrichment indicating star formation beyond the second generation. The general outline of the evolution of such a system is as follows. First, Pop III stars form (perhaps only one per minihalo) and nearly instantly enrich their surroundings with some metals. Next, a second generation of stars formed that included long-lived low-mass stars. The higher mass stars of this generation soon exploded as core collapse supernovae, while the intermediate-mass stars went through their AGB phase to release newly created elements through stellar winds. These supernova explosions were likely powerful enough to blow out gas from the shallow potential wells of these early systems, preventing further star formation. Alternatively, star formation could also have been suppressed soon after the formation of the galaxy by reionization (e.g., Lunnan et al. 2012), or both.

Low neutron-capture element abundances: evidence for one progenitor generation? All Segue 1 stars that have not been contaminated by a binary companion display an extremely low content of neutron-capture material. Considering stars with $[Fe/H] <$

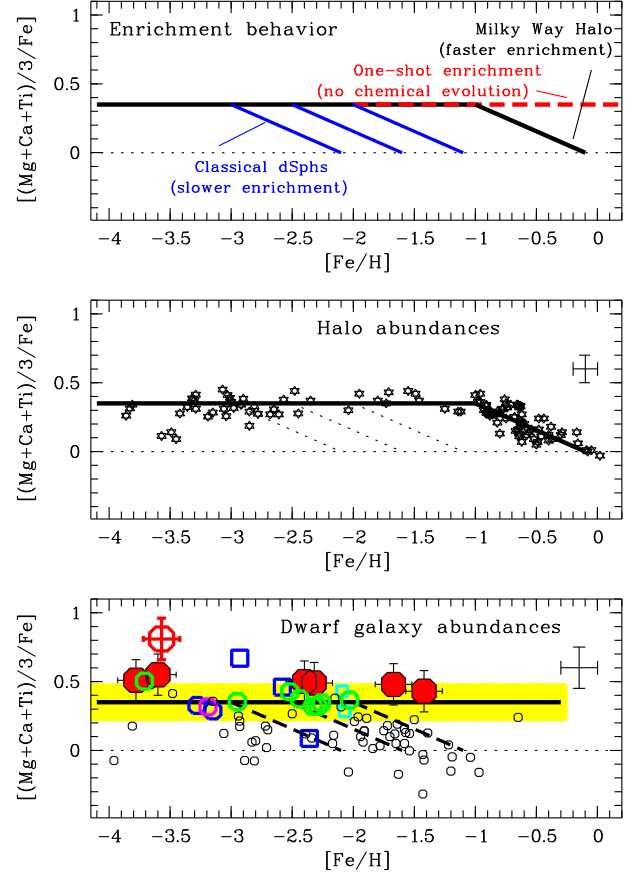


FIG. 9.— Combined Mg-Ca-Ti α -element abundances as diagnostic of early star formation, adapted from Frebel & Bromm (2012). Top: Schematic representation of chemical enrichment in the $[\alpha/Fe]$ vs $[Fe/H]$ plane for different environments. The dotted line indicates the solar ratio. Middle: High-resolution α -abundances of metal-poor stars from Cayrel et al. (2004) (halo) and Fulbright (2000) (thin/thick disk). The diagonal dotted lines indicate the enrichment behavior of the dSph galaxies (see top panel). A representative uncertainty is shown. Bottom: High-resolution α -abundances of metal-poor stars in the classical dSphs (small open black circles and several evolutionary paths are indicated with dashed lines; see Frebel & Bromm 2012 and references therein). Different colors denote different ultra-faint dwarf galaxies. Filled red circles: Segue 1 stars from this study; open red circle: Segue 1-7 (Norris et al. 2010a); blue squares: Coma Berenices; blue circles: Ursa Major II; pink circle: Leo IV; cyan squares: Hercules; green circles: Boötes I. The yellow shaded region around $[\alpha/Fe] = 0.35$ depicts the predicted Frebel & Bromm (2012) one-shot enrichment behavior (with a 0.15 dex observational uncertainty) reflecting massive core-collapse supernova enrichment.

-3 first, their $[Sr/H]$ and $[Ba/H]$ ratio upper limits and the Sr abundance measurement of Segue 1-7 equal those of the lowest ones observed in Galactic halo stars. These low abundances indicate a total amount of each neutron-capture element of no more than $\sim 10^{-7} M_{\odot}$ in Segue 1. A single neutron-capture element producing event such as an r-process supernova or a massive rotating Pop III star undergoing s-process nucleosynthesis may produce $10^{-4} M_{\odot}$ of neutron-capture elements (Farouqi et al. 2010; Pignatari et al. 2008), suggesting that at most one such event occurred during the star forming epoch in Segue 1. Hence, specific progenitor properties such as a particular mass range of supernova undergoing the r-process or perhaps an early black-hole

forming supernova with little to no neutron-capture element yields could have led to such a low overall level of neutron-capture elements in Segue 1. Deeper observations of Segue 1 stars that measure neutron-capture abundances rather than providing upper limits offer the possibility of constraining the yield of this event.

If Segue 1 is a surviving first galaxy, then no intermediate-mass AGB star enrichment signatures should be discernible in its stellar abundances. In the halo, s-process material provided by AGB stars only occurs at $[\text{Fe}/\text{H}] > -2.7$ (Simmerer et al. 2004), suggesting a corresponding characteristic neutron-capture element abundance level of $[\text{Sr}/\text{H}] > -3$ and $[\text{Ba}/\text{H}] > -3.5$. The Sr and Ba abundances in Segue 1 appear to be ~ 2 dex lower than that level even for the more metal-rich stars, confirming that AGB stars did not contribute to the enrichment of the gas cloud from which the Segue 1 stars formed.

Based on the similar high abundances of α -elements and low abundances of neutron-capture elements, it is plausible that a significant fraction of the most metal-poor halo stars ($[\text{Fe}/\text{H}] \lesssim -3$) were formed in first galaxies like Segue 1. Estimating solely from the overlap between the halo $[\text{Sr}/\text{H}]$ abundances and those in the ultra-faint dwarfs, up to half of EMP halo stars could have originated in systems with the same degree of neutron-capture element depletion. The halo stars with $[\text{Sr}/\text{H}] \gtrsim -4$ and $[\text{Ba}/\text{H}] \gtrsim -4$ likely formed in galaxies with larger stellar masses that underwent more chemical evolution with contributions from AGB stars. This picture is in qualitative agreement with that proposed by Lee et al. (2013a) to explain the difference in Ba and Sr abundance distributions between the ultra-faint dwarfs and the halo.

Interestingly, the Sr and Ba abundances of the higher metallicity Segue 1 stars are just as low as those of the extremely metal-poor stars. There are no halo stars known at $[\text{Fe}/\text{H}] \gtrsim -2.5$ that have similarly low $[\text{Sr}/\text{H}]$ and $[\text{Ba}/\text{H}]$, which means that the fraction of halo stars in this metallicity range that originated in first galaxies must be negligibly small. However, this does not mean that first galaxies cannot have contributed to the buildup of the halo at all. As described above in the Fe spread discussion, the fraction of (relatively) metal-rich stars now found in a larger galaxy like the Milky Way that formed in a first galaxy is expected to be minuscule. Their small numbers should be vastly overshadowed by the huge population of later-generation stars with similar metallicities formed in the many more-evolved dwarf galaxies that were eventually incorporated into the Galactic halo. A prediction of this scenario is that large enough surveys of the Milky Way (e.g., GALAH, Gaia) should identify a few fossil second-generation metal-rich stars with extremely low neutron-capture abundances. Assuming that the Segue 1 abundance pattern is representative of the class of first galaxies, halo stars with $[\text{Fe}/\text{H}] > -2.5$, $[\alpha/\text{H}] \geq 0.4$, $[\text{Ba}/\text{H}] \leq -4$, and $[\text{Sr}/\text{H}] \leq -5$ should be considered as candidates for having originated in a first galaxy. If such stars can be found, they would provide additional evidence for inhomogeneous mixing of metals in the earliest galaxies and the hierarchical assembly of the Galaxy from these kinds of systems.

Finally, keeping the effects of inhomogeneous metal mixing in mind, abundance spreads $[\text{X}/\text{H}]$ should be

present in all elements, not just Fe. Since we only have 3σ upper limits for $[\text{Sr}/\text{H}]$ and $[\text{Ba}/\text{H}]$ with the exception of one Sr and one Ba detection (in two different stars), we cannot make firm statements about the spread in neutron-capture element abundances in Segue 1. However, if our postulation above regarding the origin of the most neutron-capture depleted halo stars is correct, the existence of Milky Way stars at $[\text{Sr}/\text{H}] \sim -5.6$, which is ~ 0.7 dex below the lone Sr detection in Segue 1, suggests that there could be a detectable spread in neutron-capture abundances in Segue 1. The presence of a large spread in Sr and Ba is also indicated when combining the Segue 1 results with those of the most metal-poor stars in other ultra-faints such as Coma Berenices, Ursa Major II and Leo IV (Frebel et al. 2010b; Simon et al. 2010), as shown in Figure 8. However, only much higher S/N spectra of new and existing stars (which will be extremely difficult, if not impossible, to obtain with current telescopes) will allow us to conclusively test this prediction.

Segue 1 as an ancient surviving first galaxy Considering the detailed chemical abundances of the seven brightest stars in Segue 1 to describe the origin and evolution of this galaxy thus suggests that no significant chemical *evolution*, and hence star formation, has taken place in Segue 1 since its formation. There is no indication of AGB star or supernova Ia enrichment prior to the birth of any of the observed stars. It thus appears that only the first star yields have been preserved in the atmospheres of the now-observed long-lived stars. The resulting abundance pattern of similarly metal-poor halo stars closely resembles that of our Segue 1 stars, suggesting that the metal-poor tail of the Galactic metallicity distribution function might have been assembled by numerous early dwarf galaxies that produced the most metal-poor stars in their respective second or early generations of stars before additional supernovae added further metals.

The surviving first galaxy model (Frebel & Bromm 2012) predicts an ancient single-age stellar population, i.e., the long-lived part of the second generation of stars of an early galaxy that formed from minihalos in the early Universe. In terms of their chemical composition, the ultra-faint dwarfs so far all show very similar characteristics (although this conclusion is currently based on only one or a few observable stars in each galaxy). Indeed, besides Segue 1, Leo IV, Coma Berenices, and Boötes I are on the candidate first galaxy list of Frebel & Bromm (2012). Assuming Segue 1 and other ultra-faint dwarf galaxies to be surviving first galaxies then also suggests that they would need to be very old. Brown et al. (2012) and Brown et al. (2013) recently presented age measurements based on deep HST color-magnitude diagrams of three ultra-faint dwarf galaxies (Hercules, Leo IV and Ursa Major I) and preliminary results for Coma Berenices, Boötes I and Canes Venatici II. They find all of them to show very similar, single-age populations that are at least as old as the globular cluster M92 with $\sim 13 \pm 1$ Gyr.

Hence, the Brown et al. studies confirm the predicted old age of the ultra-faint dwarfs, including at least three galaxies proposed by Frebel & Bromm (2012) as surviving first galaxies and a majority of those suggested by Bovill & Ricotti (2009) as fossils (although using a different definition). While Segue 1 contains too few stars for

a robust star formation history to be derived from deep CMDs, the apparently identical stellar populations of the other ultra-faint dwarfs and the consistency of available data with the possibility of a single-age population in Segue 1 constitute strong clues that Segue 1 is similarly old and thus shows all expected signatures of a surviving first galaxy.

The History of Supernova Explosions in Segue 1

A key determinant of the early evolution of Segue 1 is how many supernova explosions it hosted during its star-forming epoch. The number of supernovae, in turn, depends on the IMF. Segue 1 does not contain enough stars for reliable IMF measurements from deep *HST* photometry (e.g., Brown et al. 2012; Geha et al. 2013), but one can nevertheless attempt an estimate. Martin et al. (2008) determined that Segue 1 contains 65 ± 9 stars brighter than $r = 22$. According to a 13 Gyr, α -enhanced, $[\text{Fe}/\text{H}] = -2.49$ isochrone from Dotter et al. (2008), this magnitude limit corresponds to a stellar mass of $0.70 M_{\odot}$, and the main sequence turnoff occurs at $0.79 M_{\odot}$. Using these numbers to set the normalization for the IMF, if the IMF above $0.5 M_{\odot}$ has the Salpeter (1955) slope of $\alpha = 2.35$ and at lower masses follows the shallower slope ($\alpha = 1.3$) determined by Kroupa et al. (1993), then the present-day stellar mass of Segue 1 from the hydrogen-burning limit up to the turnoff is $700 M_{\odot}$, and the initial stellar mass before all of the massive stars evolved was $1500 M_{\odot}$. When using such a bottom-heavy IMF, the upper mass cutoff assumed makes hardly any difference; a $50 M_{\odot}$ vs. $100 M_{\odot}$ cutoff changes the initial stellar mass by less than 4%. The total number of stars more massive than $8 M_{\odot}$ that would be expected to explode as supernovae is ~ 15 , again with little dependence on the upper mass cutoff of the IMF.

However, Geha et al. (2013) have shown that the ultra-faint dwarfs Hercules and Leo IV have a significantly bottom-light IMF for subsolar mass stars. It is not necessarily the case that the shallow power-law slope they measure for low-mass stars continued unbroken to $M > 8 M_{\odot}$ at early times, but in the absence of evidence to the contrary, it is interesting to explore the consequences of such an assumption. With the Geha et al. IMF, the stellar mass of Segue 1 today is $500 M_{\odot}$, and the initial stellar mass was $\sim 10^4 M_{\odot}$. Unlike the Kroupa case, the upper mass cut of this very top-heavy IMF has a large impact on the initial mass. Increasing the maximum mass from 50 to $100 M_{\odot}$ changes the initial mass by 50%. The number of massive stars with this top-heavy IMF is very large: ~ 300 (250 - 400 for upper mass cutoffs between 30 and $100 M_{\odot}$).

It is then interesting to investigate what the potential metal yield of these supernovae might have been. Taking the average metal mass ejected by one core-collapse supernova to be $\sim 3 M_{\odot}$ yields $900 M_{\odot}$ of metals synthesized by supernovae in Segue 1. for the Geha IMF, and $45 M_{\odot}$ of metals for the Kroupa IMF. Because the observed heavy element content of the stars in the galaxy today is $\sim 0.01 M_{\odot}$, in either case the vast majority (99.98 to 99.999%) of metals produced by Segue 1 supernovae must have been blown out of the galaxy. Such extremely efficient outflow of metals is consistent with (although more extreme than) the trends seen in more luminous dwarf galaxies by Kirby et al. (2011d). In or-

der to avoid incorporating these metals into the low-mass stars in Segue 1, this may suggest that the duration of star formation was shorter than the lifetimes of most of the massive stars (< 40 Myr), and perhaps that star formation in Segue 1 was shut off by one of the first few supernovae that occurred.

Another way of testing whether these IMF scenarios are realistic is to consider the energy deposit from supernovae to assess whether the system would be disrupted entirely. Following Whalen et al. (2008) and Johnson (2013), $< 10^7 M_{\odot}$ halos are destroyed by one massive (pair-instability) supernova with an explosion energy of 10^{53} ergs, and $10^7 M_{\odot}$ halos by 10^{54} ergs. The destruction of a more massive halo, such as a $10^8 M_{\odot}$ atomic cooling halo (a halo that can be considered a first galaxy), would require more than 10^{54} ergs.

For a typical supernova explosion of 10^{51} ergs, at least ~ 1000 supernovae would be required to disrupt even a $10^7 M_{\odot}$ halo, suggesting that Segue 1 could have survived the supernovae associated with a top-heavy IMF. This conclusion is strengthened by the fact that the abundance patterns of the most metal-poor halo stars favor “faint”, lower energy supernova explosions (Umeda & Nomoto 2003; Iwamoto et al. 2005), of 3×10^{50} ergs. Only if most of the explosions were substantially higher energy hypernovae could ~ 300 massive stars potentially destroy the galaxy. Moreover, we have assumed that the coupling of the supernova explosion energy to gas kinetic energy is 100% efficient. The coupling efficiency depends on the exact configuration of the gas, but a more reasonable order of magnitude is 10% (Thornton et al. 1998). Again, this would imply that hundreds of supernovae could have been present in Segue 1 at early times. However, even though the galaxy’s potential well was deep enough to survive a large number of supernovae, these explosions would have had dramatic effects on its gas content.

We therefore do not find any inconsistency with the hypothesis that the early-time Segue 1 could have had a top-heavy IMF, similar to what has been found for Hercules and Leo IV (Geha et al. 2013). Ultimately, more data as well as modeling of such early galaxies will hopefully reveal the nature of the IMF in these surviving ancient systems.

6. PROSPECTS AND CONCLUSION

We have presented chemical abundance measurements of six stars in the faint Segue 1 dwarf galaxy. Together with Segue 1-7 (Norris et al. 2010a), these are the brightest cool stars — and the known red giants — in Segue 1, having magnitudes around $g \sim 19$ mag. Thus, they are the only ones for which high-resolution spectra of sufficient quality can be obtained with current telescopes. Given that this sample is brightness-selected, the metallicity spread of nearly 2.5 dex is remarkable. Overall, metallicities range from $[\text{Fe}/\text{H}] = -1.4$ to $[\text{Fe}/\text{H}] = -3.8$, and three of the seven stars have $[\text{Fe}/\text{H}] \lesssim -3.5$, indicating that Segue 1 contains the highest fraction of extremely metal-poor stars ever seen.

The chemical abundances show that Segue 1 stars over the full observed metallicity range have enhanced α -element abundances at the level of metal-poor halo stars, indicating enrichment only from massive stars. Segue 1 is

the first (and only) galaxy in which no decline in $[\alpha/\text{Fe}]$ is seen at higher metallicities. The three most metal-poor stars are enhanced in carbon, also pointing to massive progenitors. The extremely small amounts of neutron-capture elements found in all Segue 1 stars point to a single neutron-capture material production event in association with massive stars, rather than AGB stars. Altogether, the abundance signature of Segue 1 agrees with predictions for Segue 1 being a surviving first galaxy that underwent only one generation of star formation after its formation from ~ 10 Pop III star hosting minihalos (Frebel & Bromm 2012).

If Segue 1 is indeed a surviving fossil, then its properties can help us understand the origin and nature of the most metal-poor stars in the Galactic halo. Specifically, simulations of the first galaxies suggest that these small, early systems could only produce extremely metal-poor stars as part of their second generation, i.e. the first generation after formation in which low-mass stars could be made. At later times, if any gas remains, it will no longer be metal-poor due to fast mixing of the metals ejected by the early supernovae. An implication of this scenario would be that many of the most metal-poor stars in the Galaxy stem from their respective first/early galaxies and are in all likelihood second generation stars. This would, to some extent, explain why it has been so difficult to model the low-metallicity tail of the halo metallicity distribution function with chemical evolution models (e.g., Schörck et al. 2009).

Following the abundance trends found in Segue 1, it appears that high $[\alpha/\text{Fe}]$ abundances together with extremely low neutron-capture abundances may be a tell-tale sign of those first galaxy second-generation stars. Many of the most metal-poor halo stars indeed share this signature with the Segue 1 stars especially at the lowest $[\text{Fe}/\text{H}]$ values. Since early inhomogeneous mixing leads to large spreads in elements $[\text{X}/\text{H}]$, the large spread in neutron-capture element abundances in the Milky Way may to some extent describe the same inhomogeneity that we observe in Segue 1 in terms of its $[\text{Fe}/\text{H}]$ spread. But instead of reflecting the content of just one galaxy, it is the superposition of spreads from the many galaxies that contributed to the build up of the metal-poor stellar population of the Galaxy.

If inhomogeneous mixing is responsible for the observed abundance spreads, the same level of scatter in neutron-capture abundance ratios should be observed in the most metal-poor stars in the classical dwarfs. Moreover, these systems should contain a relatively higher fraction of those early second generation stars than the halo. Indeed, Hercules (with $5 \times 10^4 L_\odot$) and Draco (with $4 \times 10^5 L_\odot$), are known to contain stars with unusually low neutron-capture abundances. One star in Draco at $[\text{Fe}/\text{H}] = -2.9$ has upper limits of $[\text{Sr}/\text{H}] \sim [\text{Ba}/\text{H}] < -5.5$, measured from a relatively high S/N spectrum by (Fulbright et al. 2004). It also has elevated, near halo-like $[\alpha/\text{Fe}]$ values ($[\text{Mg}/\text{Fe}] = 0.50$, $[\text{Ca}/\text{Fe}] =$

-0.07 , $[\text{Ti}/\text{Fe}] = 0.21$). The two stars in Hercules at $[\text{Fe}/\text{H}] = -2.1$ have $[\text{Sr}/\text{H}] \sim [\text{Ba}/\text{H}] < -4.2$ and similar $[\alpha/\text{Fe}]$ abundances ($[\text{Mg}/\text{Fe}] = 0.79$, $[\text{Ca}/\text{Fe}] = -0.11$, $[\text{Ti}/\text{Fe}] = 0.17$ for Her-2, and $[\text{Mg}/\text{Fe}] = 0.75$, $[\text{Ca}/\text{Fe}] = 0.21$, $[\text{Ti}/\text{Fe}] = 0.33$ for Her-3 (Koch et al. 2008).

Interestingly, no satisfactory explanations for the origin of the low neutron-capture element abundance stars in Draco and Hercules have been found until now (Fulbright et al. 2004; Koch et al. 2008). But if one were to consider these extreme stars as “left over stars” from their host system’s own building blocks one could possibly explain their existence by assuming that systems with $\sim 10^5 L_\odot$ and more are already “assembled galaxies” themselves. If systems like Draco show true second-generation stars (here taken to have very low neutron-capture element abundances) from their respective first galaxy building blocks at a rate of only 1 in 15 (based on the observed sample of stars in Draco; Shetrone et al. 2001; Fulbright et al. 2004; Cohen & Huang 2009), then it could be understood why no such stars have yet been found in the even more luminous classical dwarf galaxies, and especially the halo.

These dwarf spheroidal galaxies also show declining α -abundances with increasing metallicity (Kirby et al. 2011a). These higher metallicity stars must be from later stellar generations which presumably after mergers with additional of their building blocks or after significant gas accretion and retention. Broadly speaking, the lower α -abundance stars reflect later-time enrichment by supernova Ia (e.g., Shetrone et al. 2001) although other scenarios may be able to explain the observations of the stellar content of these dwarfs as well. Detailed analyses of more stars at all metallicities, but particularly at high metallicity in the ultra-faint dwarfs and at low-metallicity in the classical dwarfs, will reveal more about the assembly histories of dwarf galaxies as well as the formation of the halo of the Milky Way.

We thank Andrew McWilliam for providing the Arcturus spectrum. A.F. is supported by NSF CAREER grant AST-1255160. J.D.S. is supported by NSF grant AST-1108811. E.N.K. acknowledges support from the Southern California Center for Galaxy Evolution, a multicampus research program funded by the University of California Office of Research. This work made use of the NASA’s Astrophysics Data System Bibliographic Services.

We are grateful to the many people who have worked to make the Keck Telescope and its instruments a reality and to operate and maintain the Keck Observatory. The and to operate and maintain the Keck Observatory. The authors wish to extend special thanks to those of Hawaiian ancestry on whose sacred mountain we are privileged to be guests. Without their generous hospitality, none of the observations presented herein would have been possible.

Facilities: Magellan-Clay (MIKE), Keck:I (HIRES)

REFERENCES

- Aoki, W., Beers, T. C., Christlieb, N., et al. 2007, *ApJ*, 655, 492
- Aoki, W., Honda, S., Beers, T. C., et al. 2005, *ApJ*, 632, 611
- Aoki, W., Norris, J. E., Ryan, S. G., Beers, T. C., & Ando, H. 2002a, *ApJ*, 576, L141
- . 2002b, *ApJ*, 567, 1166
- Asplund, M., Grevesse, N., Sauval, A. J., & Scott, P. 2009, *ARA&A*, 47, 481
- Barklem, P. S., Christlieb, N., Beers, T. C., et al. 2005, *A&A*, 439, 129
- Baummueller, D., Butler, K., & Gehren, T. 1998, *A&A*, 338, 637

TABLE 5
 MAGELLAN/MIKE CHEMICAL ABUNDANCES OF ALL SEGUE 1
 STARS

Species	<i>N</i>	$\log \epsilon(X)$	σ	[X/H]	[X/Fe]
SDSS J100714+160154					
CH	1	8.45	0.20	0.02	1.44
Na I	2	4.79	0.12	-1.46	-0.04
Mg I	7	6.56	0.18	-1.04	0.38
Al I	2	4.37	0.20	-2.08	-0.66
Si I	1	6.48	0.15	-1.03	0.39
Ca I	22	5.36	0.13	-0.98	0.44
Sc II	2	1.68	0.17	-1.47	-0.05
Ti I	25	3.84	0.11	-1.11	0.31
Ti II	28	4.01	0.10	-0.94	0.48
Cr I	16	4.21	0.19	-1.43	-0.02
Cr II	2	4.68	0.10	-0.96	0.46
Mn I	5	3.51	0.21	-1.92	-0.50
Fe I	187	6.08	0.24	-1.42	0.00
Fe II	23	6.08	0.18	-1.42	-0.00
Co I	4	3.65	0.17	-1.34	0.08
Ni I	10	4.79	0.12	-1.43	-0.01
Zn I	2	3.29	0.22	-1.27	0.15
Sr II	1	2.35	0.20	-0.52	0.90
Zr II	1	2.56	0.25	-0.02	1.40
Ba II	3	2.61	0.18	0.43	1.85
La II	1	1.48	0.25	0.38	1.80
Eu II	3	-0.17	0.14	-0.69	0.73
Pb I	1	2.30	0.50	0.55	1.97
SDSS J100710+160623					
CH	2	6.91	0.20	-1.52	0.15
Na I	2	4.31	0.10	-1.93	-0.26
Mg I	5	6.39	0.10	-1.21	0.47
Al I	1	3.88	0.25	-2.57	-0.90
Si I	1	6.37	0.15	-1.14	0.53
Ca I	25	5.25	0.23	-1.09	0.58
Sc II	7	1.61	0.12	-1.54	0.13
Ti I	26	3.66	0.15	-1.29	0.38
Ti II	39	3.65	0.15	-1.30	0.38
Cr I	17	3.84	0.16	-1.80	-0.13
Cr II	1	3.76	0.15	-1.88	-0.21
Mn I	6	3.27	0.15	-2.16	-0.49
Fe I	210	5.83	0.22	-1.67	0.00
Fe II	23	5.85	0.18	-1.65	0.02
Co I	5	3.32	0.07	-1.67	0.00
Ni I	14	4.56	0.16	-1.66	0.01
Zn I	1	<2.84	...	<-1.72	<-0.05
Sr II	1	<-2.00	...	<-4.87	<-3.20
Ba II	1	<-2.10	...	<-4.28	<-2.61
Eu II	1	<-1.15	...	<-1.67	<0.00
SDSS J100702+155055					
CH	2	6.19	0.20	-2.24	0.08
Na I	2	4.07	0.14	-2.17	0.15
Mg I	8	5.80	0.12	-1.80	0.52
Al I	2	3.29	0.20	-3.16	-0.84
Si I	2	5.60	0.15	-1.90	0.42
Ca I	19	4.53	0.11	-1.81	0.51
Sc II	5	0.93	0.15	-2.22	0.10
Ti I	11	3.01	0.11	-1.94	0.38
Ti II	35	3.05	0.17	-1.90	0.43
Cr I	10	3.17	0.09	-2.47	-0.15
Mn I	7	2.54	0.15	-2.87	-0.57
Fe I	162	5.18	0.18	-2.32	0.00
Fe II	15	5.18	0.15	-2.32	0.00
Co I	2	2.57	0.10	-2.42	-0.10
Ni I	5	3.79	0.23	-2.43	-0.11
Zn I	1	<2.69	...	<-1.87	<0.45
Sr II	1	<-2.19	...	<-5.06	<-2.74
Ba II	1	<-2.26	...	<-4.44	<-2.12
Eu II	1	<-1.50	...	<-2.02	<0.30

^a [X/H] and [X/Fe] values have been recalculated from log gf values using the Asplund et al. (2009) solar abundances.

 TABLE 6
 TABLE 5 CONTINUED – MAGELLAN/MIKE CHEMICAL
 ABUNDANCES OF ALL SEGUE 1 STARS

Species	<i>N</i>	$\log \epsilon(X)$	σ	[X/H]	[X/Fe]
SDSS J100742+160106					
CH	2	5.93	0.20	-2.50	-0.10
Na I	2	3.61	0.10	-2.63	-0.23
Mg I	7	5.74	0.08	-1.86	0.54
Al I	2	3.38	0.15	-3.07	-0.67
Si I	1	5.74	0.15	-1.77	0.63
Ca I	21	4.46	0.09	-1.88	0.52
Sc II	6	1.06	0.10	-2.09	0.31
Ti I	16	2.95	0.10	-2.00	0.40
Ti II	33	3.00	0.13	-1.95	0.45
Cr I	9	2.96	0.17	-2.68	-0.28
Mn I	4	2.61	0.25	-2.82	-0.42
Fe I	170	5.10	0.17	-2.40	0.00
Fe II	17	5.11	0.10	-2.39	0.01
Co I	2	2.72	0.14	-2.27	0.13
Ni I	1	3.95	0.15	-2.27	0.13
Zn I	1	<2.47	...	<-2.09	<0.31
Sr II	1	<-2.30	...	<-5.17	<-2.77
Ba II	1	-2.20	0.20	-4.38	-1.98
Eu II	1	<-1.40	...	<-1.92	<0.48
SDSS J100652+160235					
CH	2	6.03	0.20	-2.40	1.20
Na I	2	2.75	0.10	-3.49	0.11
Mg I	6	4.59	0.06	-3.01	0.59
Al I	1	2.25	0.20	-4.20	-0.60
Si I	1	4.31	0.15	-3.19	0.41
Ca I	3	3.30	0.13	-3.04	0.56
Sc II	1	-0.10	0.15	-3.25	0.35
Ti II	12	1.95	0.14	-3.00	0.60
Cr I	1	1.72	0.15	-3.92	-0.32
Mn I	1	<1.50	...	<-3.93	<-0.33
Fe I	47	3.90	0.23	-3.60	0.00
Co I	2	1.91	0.10	-3.08	0.52
Ni I	4	2.75	0.15	-3.47	0.13
Zn I	1	<2.40	...	<-2.16	<1.44
Sr II	1	<-1.63	...	<-4.50	<-0.90
Ba II	1	<-1.87	...	<-4.05	<-0.45
Eu II	1	<-1.08	...	<-1.60	<2.00
SDSS J100639+160008					
CH	2	5.56	0.25	-2.87	0.91
Na I	2	2.74	0.10	-3.50	0.28
Mg I	4	4.40	0.10	-3.20	0.57
Al I	2	1.98	0.25	-4.47	-0.70
Si I	1	5.00	0.25	-2.51	1.27
Ca I	2	3.16	0.10	-3.18	0.59
Sc II	2	-0.65	0.10	-3.80	-0.02
Ti II	12	1.55	0.18	-3.40	0.37
Cr I	3	1.44	0.16	-4.20	-0.42
Mn I	2	1.10	0.10	-4.33	-0.55
Fe I	35	3.72	0.11	-3.78	0.00
Co I	2	1.61	0.10	-3.38	0.40
Ni I	3	2.59	0.12	-3.63	0.15
Zn I	1	<2.04	...	<-2.52	<1.26
Sr II	1	<-2.21	...	<-5.08	<-1.30
Ba II	1	<-2.25	...	<-4.43	<-0.65
Eu II	1	<-1.26	...	<-1.78	<2.00
Segue 1-7 (from Norris et al. 2010a) ^a					
CH	2	7.17	0.20	-1.26	2.31
Na I	2	3.18	0.04	-3.06	0.51
Mg I	5	4.95	0.07	-2.65	0.92
Al I	1	3.08	...	-3.37	0.20
Si I	1	4.79	0.20	-2.72	0.85
Ca I	9	3.63	0.04	-2.71	0.86
Sc II
Ti II	11	2.03	0.08	-2.92	0.65
Cr I	3	1.86	0.05	-3.78	-0.21
Mn I	1	1.31	...	-4.12	-0.55
Fe I	37	3.93	0.03	-3.57	0.00
Co I	4	1.77	0.15	-3.22	0.35
Ni I	1	2.16	...	-4.06	-0.49
Zn I
Sr II	2	-1.99	0.23	-4.86	-1.29
Ba II	1	<-2.31	...	<-4.49	<-0.92
Eu II	1	<-2.20	...	<-2.72	<0.85

^a [X/H] and [X/Fe] values have been recalculated from log gf values using the Asplund et al. (2009) solar abundances.

- Beers, T. C., & Christlieb, N. 2005, *ARA&A*, 43, 531
- Belokurov, V., Zucker, D. B., Evans, N. W., et al. 2007, *ApJ*, 654, 897
- Bernstein, R., Shectman, S. A., Gunnels, S. M., Mochnacki, S., & Athey, A. E. 2003, in *Society of Photo-Optical Instrumentation Engineers (SPIE) Conference Series*, ed. M. Iye & A. F. M. Moorwood, Vol. 4841, 1694
- Bovill, M. S., & Ricotti, M. 2009, *ApJ*, 693, 1859
- . 2011, *ApJ*, 741, 17
- Bromm, V., & Loeb, A. 2003, *Nature*, 425, 812
- Brown, T. M., Tumlinson, J., Geha, M., et al. 2012, *ApJ*, 753, L21
- . 2013, *arXiv:1310.0824*
- Brusadin, G., Matteucci, F., & Romano, D. 2013, *A&A*, 554, A135
- Burris, D. L., Pilachowski, C. A., Armandroff, T. E., et al. 2000, *ApJ*, 544, 302
- Carretta, E., D'Orazi, V., Gratton, R. G., & Lucatello, S. 2012, *A&A*, 543, A117
- Castelli, F., & Kurucz, R. L. 2004, *arXiv:astro-ph/0405087*
- Cayrel, R., Depagne, E., Spite, M., et al. 2004, *A&A*, 416, 1117
- Chiappini, C., Frischknecht, U., Meynet, G., et al. 2011, *Nature*, 472, 454
- Clem, J. L., Vanden Berg, D. A., & Stetson, P. B. 2008, *AJ*, 135, 682
- Cohen, J. G., & Huang, W. 2009, *ApJ*, 701, 1053
- Cohen, J. G., McWilliam, A., Shectman, S., et al. 2006, *AJ*, 132, 137
- Dotter, A., Chaboyer, B., Jevremović, D., et al. 2008, *ApJS*, 178, 89
- Edvardsson, B., Andersen, J., Gustafsson, B., et al. 1993, *A&A*, 275, 101
- Farouqi, K., Kratz, K.-L., Pfeiffer, B., et al. 2010, *ApJ*, 712, 1359
- François, P., Depagne, E., Hill, V., et al. 2007, *A&A*, 476, 935
- François, P., Monaco, L., Villanova, S., et al. 2012, in *American Institute of Physics Conference Series*, Vol. 1484, American Institute of Physics Conference Series, ed. S. Kubono, T. Hayakawa, T. Kajino, H. Miyatake, T. Motobayashi, & K. Nomoto, 460–462
- Frebel, A. 2010, *Astronomische Nachrichten*, 331, 474
- Frebel, A., & Bromm, V. 2012, *ApJ*, 759, 115
- Frebel, A., Casey, A. R., Jacobson, H. R., & Yu, Q. 2013a, *ApJ*, 769, 57
- Frebel, A., Christlieb, N., Norris, J. E., et al. 2006a, *ApJ*, 652, 1585
- Frebel, A., Christlieb, N., Norris, J. E., Aoki, W., & Asplund, M. 2006b, *ApJ*, 638, L17
- Frebel, A., Johnson, J. L., & Bromm, V. 2007a, *MNRAS*, 380, L40
- Frebel, A., Kirby, E. N., & Simon, J. D. 2010a, *Nature*, 464, 72
- Frebel, A., Lunnan, R., Casey, A. R., et al. 2013b, *ApJ*, 771, 39
- Frebel, A., & Norris, J. E. 2013, *Metal-Poor Stars and the Chemical Enrichment of the Universe*, ed. T. D. Oswalt & G. Gilmore, 55
- Frebel, A., Norris, J. E., Aoki, W., et al. 2007b, *ApJ*, 658, 534
- Frebel, A., Simon, J. D., Geha, M., & Willman, B. 2010b, *ApJ*, 708, 560
- Fulbright, J. P., Rich, R. M., & Castro, S. 2004, *ApJ*, 612, 447
- Geha, M., Brown, T. M., Tumlinson, J., et al. 2013, *ApJ*, 771, 29
- Geha, M., Willman, B., Simon, J. D., et al. 2009, *ApJ*, 692, 1464
- Green, E. M., Demarque, P., & King, C. R. 1984, *BAAS*, 16, 997
- Greif, T., Springel, V., White, S., et al. 2011, *arXiv:1101.5491*
- Hollek, J. K., Frebel, A., Roederer, I. U., et al. 2011, *ApJ*, 742, 54
- Iwamoto, N., Umeda, H., Tominaga, N., Nomoto, K., & Maeda, K. 2005, *Science*, 309, 451
- Jacobson, H. R., & Frebel, A. 2013, *arXiv:1309.0037*
- Johnson, J. L. 2013, in *Astrophysics and Space Science Library*, Vol. 396, *Astrophysics and Space Science Library*, ed. T. Wiklund, B. Mobasher, & V. Bromm, 177
- Karakas, A. I. 2010, *MNRAS*, 403, 1413
- Kelson, D. D. 2003, *PASP*, 115, 688
- Kim, Y.-C., Demarque, P., Yi, S. K., & Alexander, D. R. 2002, *ApJS*, 143, 499
- Kirby, E. N., Cohen, J. G., Guhathakurta, P., et al. 2013, *arXiv:1310.0814*
- Kirby, E. N., Cohen, J. G., Smith, G. H., et al. 2011a, *ApJ*, 727, 79
- Kirby, E. N., Lanfranchi, G. A., Simon, J. D., Cohen, J. G., & Guhathakurta, P. 2011b, *ApJ*, 727, 78
- . 2011c, *ApJ*, 727, 78
- Kirby, E. N., Martin, C. L., & Finlator, K. 2011d, *ApJ*, 742, L25
- Kirby, E. N., Simon, J. D., Geha, M., Guhathakurta, P., & Frebel, A. 2008, *ApJ*, 685, L43
- Koch, A., Feltzing, S., Adén, D., & Matteucci, F. 2013, *A&A*, 554, A5
- Koch, A., McWilliam, A., Grebel, E. K., Zucker, D. B., & Belokurov, V. 2008, *ApJ*, 688, L13
- Kroupa, P., Tout, C. A., & Gilmore, G. 1993, *MNRAS*, 262, 545
- Krumholz, M. R., & Tan, J. C. 2007, *ApJ*, 654, 304
- Lai, D. K., Bolte, M., Johnson, J. A., et al. 2008, *ApJ*, 681, 1524
- Lee, D. M., Johnston, K. V., Tumlinson, J., Sen, B., & Simon, J. D. 2013a, *ApJ*, 774, 103
- Lee, Y. S., Beers, T. C., Masseron, T., et al. 2013b, *AJ*, 146, 132
- Lemasle, B., Hill, V., Tolstoy, E., et al. 2012, *A&A*, 538, A100
- Letarte, B., Hill, V., Tolstoy, E., et al. 2010, *A&A*, 523, A17
- Lucatello, S., Beers, T. C., Christlieb, N., et al. 2006, *ApJ*, 652, L37
- Lugaro, M., Karakas, A. I., Stancliffe, R. J., & Rijs, C. 2012, *ApJ*, 747, 2
- Lunnan, R., Vogelsberger, M., Frebel, A., et al. 2012, *ApJ*, 746, 109
- Maoz, D., & Mannucci, F. 2012, *PASA*, 29, 447
- Martin, N. F., de Jong, J. T. A., & Rix, H.-W. 2008, *ApJ*, 684, 1075
- Martinez, G. D., Minor, Q. E., Bullock, J., et al. 2011, *ApJ*, 738, 55
- Masseron, T., Johnson, J. A., Plez, B., et al. 2010, *A&A*, 509, A93
- McWilliam, A. 1997, *ARA&A*, 35, 503
- McWilliam, A., Preston, G. W., Sneden, C., & Searle, L. 1995, *AJ*, 109, 2757
- McWilliam, A., Wallerstein, G., & Mottini, M. 2013, *ApJ*, 778, 149
- Meynet, G., Ekström, S., & Maeder, A. 2006, *A&A*, 447, 623
- Niederste-Ostholt, M., Belokurov, V., Evans, N. W., et al. 2009, *MNRAS*, 398, 1771
- Norris, J. E., Gilmore, G., Wyse, R. F. G., Yong, D., & Frebel, A. 2010a, *ApJ*, 722, L104
- Norris, J. E., Wyse, R. F. G., Gilmore, G., et al. 2010b, *ApJ*, 723, 1632
- Norris, J. E., Yong, D., Gilmore, G., & Wyse, R. F. G. 2010c, *ApJ*, 711, 350
- Okamoto, S., Arimoto, N., Yamada, Y., & Onodera, M. 2012, *ApJ*, 744, 96
- Pignatari, M., Gallino, R., Meynet, G., et al. 2008, *ApJL*, 687, L95
- Placco, V. M., Frebel, A., Beers, T. C., et al. 2013, *ApJ*, 770, 104
- Preston, G. W., Sneden, C., Thompson, I. B., Shectman, S. A., & Burley, G. S. 2006, *AJ*, 132, 85
- Robin, A. C., Reylé, C., Derrière, S., & Picaud, S. 2003, *A&A*, 409, 523
- Roederer, I. U. 2013, *AJ*, 145, 26
- Roederer, I. U., Frebel, A., Shetrone, M. D., et al. 2008, *ApJ*, 679, 1549
- Rossi, S., Beers, T. C., & Sneden, C. 1999, in *ASP Conf. Ser. 165: The Third Stromlo Symposium: The Galactic Halo*, 264
- Salpeter, E. E. 1955, *ApJ*, 121, 161
- Schörck, T., Christlieb, N., Cohen, J. G., et al. 2009, *A&A*, 507, 817
- Shetrone, M. D., Côté, P., & Sargent, W. L. W. 2001, *ApJ*, 548, 592
- Simmerer, J., Sneden, C., Cowan, J. J., et al. 2004, *ApJ*, 617, 1091
- Simon, J. D., Frebel, A., McWilliam, A., Kirby, E. N., & Thompson, I. B. 2010, *ApJ*, 716, 446
- Simon, J. D., & Geha, M. 2007, *ApJ*, 670, 313
- Simon, J. D., Geha, M., Minor, Q. E., et al. 2011, *ApJ*, 733, 46
- Sneden, C. A. 1973, *PhD thesis*, The University of Texas at Austin
- Sobeck, J. S., Kraft, R. P., Sneden, C., et al. 2011, *AJ*, 141, 175
- Thornton, K., Gaudlitz, M., Janka, H.-T., & Steinmetz, M. 1998, *ApJ*, 500, 95
- Tinsley, B. M. 1979, *ApJ*, 229, 1046
- Tissera, P. B., White, S. D. M., & Scannapieco, C. 2012, *MNRAS*, 420, 255
- Tolstoy, E., Hill, V., & Tosi, M. 2009, *ARA&A*, 47, 371
- Tolstoy, E., Venn, K. A., Shetrone, M., et al. 2003, *AJ*, 125, 707
- Umeda, H., & Nomoto, K. 2003, *Nature*, 422, 871

- Vargas, L. C., Geha, M., Kirby, E. N., & Simon, J. D. 2013, *ApJ*, 767, 134
- Venn, K. A., Irwin, M., Shetrone, M. D., et al. 2004, *AJ*, 128, 1177
- Vogt, S. S., Allen, S. L., Bigelow, B. C., et al. 1994, in *Society of Photo-Optical Instrumentation Engineers Conf. Ser.*, ed. D. L. Crawford & E. R. Craine, Vol. 2198, 362
- Whalen, D., van Veelen, B., O’Shea, B. W., & Norman, M. L. 2008, *ApJ*, 682, 49
- Willman, B., Dalcanton, J. J., Martinez-Delgado, D., et al. 2005, *ApJ*, 626, L85
- Woosley, S. E., & Weaver, T. A. 1995, *ApJS*, 101, 181
- Yong, D., Grundahl, F., Nissen, P. E., Jensen, H. R., & Lambert, D. L. 2005, *A&A*, 438, 875
- Yong, D., Norris, J. E., Bessell, M. S., et al. 2013, *ApJ*, 762, 26
- Zolotov, A., Willman, B., Brooks, A. M., et al. 2009, *ApJ*, 702, 1058
- . 2010, *ApJ*, 721, 738
- Zucker, D. B., Belokurov, V., Evans, N. W., et al. 2006, *ApJ*, 643, L103